

NAVAL POSTGRADUATE SCHOOL

Monterey, California



THESIS

TELEMETRY AND GPS ANTENNAS FOR A MICRO AIR VEHICLE

By

Emin Guven

September 1999

Thesis Advisor :
Second Reader:

David C. Jenn
D. Curtis Schleher

Approved for public release; distribution is unlimited.

DTIC QUALITY INSPECTED 4

19991022 169

REPORT DOCUMENTATION PAGE			Form Approved OMB No. 0704-0188	
<p>Public reporting burden for this collection of information is estimated to average 1 hour per response, including the time for reviewing instruction, searching existing data sources, gathering and maintaining the data needed, and completing and reviewing the collection of information. Send comments regarding this burden estimate or any other aspect of this collection of information, including suggestions for reducing this burden, to Washington Headquarters Services, Directorate for Information Operations and Reports, 1215 Jefferson Davis Highway, Suite 1204, Arlington, VA 22202-4302, and to the Office of Management and Budget, Paperwork Reduction Project (0704-0188) Washington DC 20503.</p>				
1. AGENCY USE ONLY (Leave blank)		2. REPORT DATE September 1999		3. REPORT TYPE AND DATES COVERED Master's Thesis
4. TITLE AND SUBTITLE Telemetry and GPS Antennas for A Micro Air Vehicle.			5. FUNDING NUMBERS	
6. AUTHOR(S) Guven, Emin				
7. PERFORMING ORGANIZATION NAME(S) AND ADDRESS(ES) Naval Postgraduate School Monterey, CA 93943-5000			8. PERFORMING ORGANIZATION REPORT NUMBER	
9. SPONSORING/MONITORING AGENCY NAME(S) AND ADDRESS(ES)			10. SPONSORING/MONITORING AGENCY REPORT NUMBER	
11. SUPPLEMENTARY NOTES The views expressed in this thesis are those of the author and do not reflect the official policy or position of the Department of Defense or the U.S. Government.				
12a. DISTRIBUTION/AVAILABILITY STATEMENT Approved for public release; distribution is unlimited.			12b. DISTRIBUTION CODE	
13. ABSTRACT (<i>maximum 200 words</i>) This thesis presents telemetry and GPS antenna designs for a Micro Air Vehicle (MAV). The telemetry antenna type is selected as a monopole, which is to be mounted under the bottom of MAV. A prototype of the telemetry antenna was designed, built, and tested at 2.45 GHz. For the GPS antenna, several types of antennas were examined. Helix, conical spiral, tripole, and crossed-dipole antenna types were designed and simulated using computer software. Additionally, microstrip and slotted-ring antenna types were presented. The antenna computations were performed using the Numerical Electromagnetics Code (NEC).				
14. SUBJECT TERMS GPS Antennas, Telemetry Antennas, Micro Air Vehicle, NEC.			15. NUMBER OF PAGES 79	
			16. PRICE CODE	
17. SECURITY CLASSIFICATION OF REPORT Unclassified	18. SECURITY CLASSIFICATION OF THIS PAGE Unclassified	19. SECURITY CLASSIFICATION OF ABSTRACT Unclassified	20. LIMITATION OF ABSTRACT UL	

Approved for public release; distribution is unlimited.

**TELEMETRY AND GPS ANTENNAS
FOR A MICRO AIR VEHICLE**

Emin Guven
Lieutenant Junior Grade, Turkish Navy
B.S., Turkish Naval Academy, Istanbul, 1993

Submitted in partial fulfillment of the
requirements for the degree of

MASTER OF SCIENCE IN SYSTEMS ENGINEERING

from the

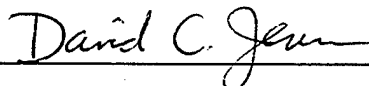
**NAVAL POSTGRADUATE SCHOOL
September 1999**

Author:




Emin Guven

Approved by:



David C. Jenn, Thesis Advisor



D. Curtis Schleher, Second Reader



Dan C. Boger, Chairman
Information Warfare Academic Group

ABSTRACT

This thesis presents telemetry and GPS antenna designs for a Micro Air Vehicle (MAV). The telemetry antenna type is selected as a monopole, which is to be mounted under the bottom of MAV. A prototype of the telemetry antenna was designed, built, and tested at 2.45 GHz. For the GPS antenna, several types of antennas were examined. Helix, conical spiral, tripole, and crossed-dipole antenna types were designed and simulated using computer software. Additionally, microstrip and slotted-ring antenna types were presented. The antenna computations were performed using the Numerical Electromagnetics Code (NEC).

TABLE OF CONTENTS

I.	INTRODUCTION.....	1
	A. BACKGROUND.....	1
	B. APPROACH.....	4
II.	FUNDAMENTAL DESIGN PARAMETERS OF ANTENNAS.....	7
	A. INTRODUCTION.....	7
	B. ANTENNA IMPEDANCE.....	8
	C. RADIATION PATTERN	9
	D. POLARIZATION.....	10
	E. DIRECTIVITY AND GAIN.....	11
	F. VOLTAGE STANDING WAVE RATIO (VSWR).....	13
III.	COMPUTER CODE DESCRIPTION	15
IV.	TELEMETRY ANTENNA.....	17
	A. INTRODUCTION.....	17
	B. COMPUTER SIMULATION	18
	C. PROTOTYPE OF THE TELEMETRY ANTENNA.....	21
V.	GPS ANTENNA	27
	A. INTRODUCTION.....	27
	B. MICROSTRIP PATCH ANTENNA.....	30
	C. HELIX ANTENNA.....	32
	D. CONICAL SPIRAL ANTENNA	36
	E. TRIPOLE ANTENNA	37
	F. CROSSED-DIPOLE ANTENNA	39
	G. SLOTTED-RING ANTENNA.....	43
VI.	CONCLUSION	45
	APPENDIX A NEC-WIN INPUT FILES.....	49
	APPENDIX B MATLAB PROGRAM FILE	57
	LIST OF REFERENCES	65
	INITIAL DISTRIBUTION LIST	67

ACKNOWLEDGEMENT

I would like to thank Prof. David C. Jenn for his technical expertise and supervision.
I will always appreciate his patience and clarity.

I also want to thank Robert Vitale for his technical assistance during building and testing phases in NPS Microwave Laboratory.

I. INTRODUCTION

A. BACKGROUND

Unmanned air vehicles (UAVs) have been used for many years. The concept of a very small UAV, referred to as a micro air vehicle (MAV), has been proposed for many applications [Refs. 1-2].

UAVs generally have been used for military purposes precisely because they are unmanned vehicles, and pilots, who are especially important in wartime situations, are not assigned for dangerous missions. Naturally, UAVs are built much smaller than the manned vehicles because they do not require the pilot and the pilot support systems. UAVs are flying robots, which can deploy a useful micro payload to a remote or otherwise hazardous location where it may perform any of a variety of tactical missions. General application purposes of military UAVs are photo reconnaissance, electronic intelligence gathering, bomb damage assessment, psychological warfare (propaganda leaflet dropping), and electronic warfare. The UAVs can also conduct some missions for civil uses such as fire detection and wildfire mapping, fishing and law enforcement, security of high-value property, pipeline patrol, storm research, detection and sensing of radiation as well as chemical or biological contamination, and various agriculture duties.

The most important factor for UAV's success mainly depends on the sensors and other electronic devices that are mounted on it. Cameras, forward-looking infrared radar (FLIR), and communications equipment for vehicle-to-ground data links can be miniaturized and built into the air vehicle. Such a small vehicle is covert; it is so small that it is stealthy with regard to radar, infrared, and visual detection.

The main difference between the general UAVs and the MAVs can be explained simply in terms of size. The prefix micro refers to their small size [Ref. 1]. They are considered as fully functional and affordable small flight vehicles, which can be used in combat operations for military purposes. The size of a MAV as defined by the Defense Advanced Research Projects Agency (DARPA) is a vehicle less than 15 cm (about 6 inches) in length, width or height [Ref. 2]. The small size of the MAV brings severely constrained weight and volume limitations.

Studies like the Defense Science Board's 1996 Summer Study on "Tactics and Technologies for 21st Century Warfighting" [Ref. 2] emphasize keeping personnel out of harm's way by providing unprecedented situational awareness right down to the platoon level. In contrast to higher-level reconnaissance assets like satellites and high altitude UAVs, MAVs will be operated by and for the individual soldier in the field as a platoon-level asset, providing local reconnaissance or other sensor information on demand, where and when it is needed. MAVs may also be used for tagging, targeting, and communications, and may eventually find application as weapons, as well. The current concept suggests that reconnaissance MAVs need a range out to perhaps 10 km, remain aloft for up to 2 hours, reach speeds of 10 to 20 m/s (22 to 45 mph), and be capable of real time day/night imagery. In contrast, some surveillance applications may require less range-payload performance. In these instances, the MAV would relocate to a suitable vantage point and serve as a fixed, unattended surface sensor with capabilities ranging from imagery to seismic detection [Ref. 2].

Power must be provided for the MAV propulsion and to operate the systems on board. With regard to the power problem, there is nothing more effective than reducing

weight in order to reduce the power requirements. Technologies like MEMS, low power electronics, and component multifunctionality will help. High energy density (i.e., lightweight) power sources are essential. Gasoline or battery based systems will likely power the first generation MAVs, but more exotic technologies like fuel cells are being developed for follow-on systems [Ref. 2].

Success in any MAV mission rests with ability to establish a successful, robust communications link between the MAV and its user/operator. Communication problems relate primarily to the small vehicle size, hence small antenna size, and to the limited power available to support the bandwidth required (2-4 megabits per second) for image transmission. Control functions demand much lower bandwidth capabilities (in the 10s of kilobits range). Image compression helps reduce the bandwidth requirement, but this increases on-board processing and hence power requirements. The limited power budget means the omni-directional signal will be quite weak, so directional ground antennas will be required to track the vehicle using line-of-sight transmissions. However, limitations to line-of-sight would be severely restrictive for urban operations, so other approaches will have to be found. One approach is to explore cellular communication architectures [Ref. 2].

The demonstration models currently under development by DARPA are required to send video data back to the pilot as well as receive command and control signals from the pilot. Therefore, the first generation gas-powered version of MAV requires a transmitter and a telemetry antenna on the vehicle to transmit the video data to the ground station. The most important requirements are that the antenna be lightweight and have nearly isotropic coverage [Ref. 3].

In many applications, accurate position information will be required. A global positioning system (GPS) receiver and antenna on board will serve this purpose. The GPS antenna must have an unobstructed view of satellites from the horizon to zenith.

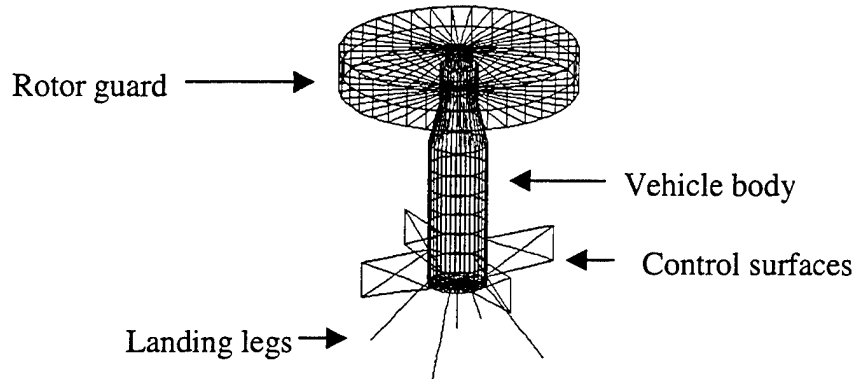


Figure 1.1 Typical rotorcraft micro air vehicle configuration.

B. APPROACH

Most of the rotorcraft MAV design concepts involve a cylindrical body, which encloses the gas engine, transmitter, control electronics, and the video camera (see Figure 1.1). In this thesis the cylindrical body is considered as the baseline approach. The main research purpose of this thesis is to design, test, and build the telemetry antenna and investigate several types of GPS antennas. The antennas are designed with the help of a computational electromagnetics code. For design purposes, NEC-Win Professional (NEC-Win) electromagnetics simulation program is used to predict the radiation pattern as a function of several design parameters.

The proposed telemetry antenna is a monopole to be mounted just under the bottom of the cylindrical body. The primary design criteria are a broad radiation pattern and an input impedance of 50 Ohms. For the GPS antenna, microstrip patch, helix, conical spiral, tripole, crossed-dipole, and slotted-ring antenna types are considered. A single microstrip patch antenna would have to be mounted on the top of the rotor hub.

Alternately two side-looking patches could be mounted on opposite sides of the body. A helix antenna could be conformed to the cylindrical body. The conical spiral antenna could be mounted under the cylindrical body replacing legs while the crossed-dipole antenna could be designed into the landing legs of the MAV. The tripole antenna would be mounted around the cylindrical body of the MAV near the bottom of the structure. A slotted-ring antenna could be wound around the cylindrical lower body of the MAV. Upon completion of design processes by using NEC-Win, the candidate antenna types and their advantages and disadvantages are presented.

Chapter II of the thesis reviews some antenna theory and its important parameters such as antenna impedance, radiation pattern, polarization, directivity, gain and voltage standing wave ratio (VSWR). Chapter III gives a brief description of the simulation tool and its capabilities. Chapter IV outlines the design, test, and building phases of the telemetry antenna. Chapter V addresses the various GPS antenna configurations for MAV and shows the design and test results for those types of GPS antennas. Chapter VI presents conclusions and recommendations for future research. The NEC-Win input files used for the designs of telemetry and GPS antennas in this thesis are included in APPENDIX A. A sample of MATLAB code used for the drawings of the radiation patterns for the antennas is presented in APPENDIX B.

THIS PAGE INTENTIONALLY LEFT BLANK

II. FUNDAMENTAL DESIGN PARAMETERS OF ANTENNAS

A. INTRODUCTION

The antenna is defined as “a means for radiating or receiving radio waves” in the *IEEE Standard Definitions of Terms for Antennas* (IEEE Std 145-1973) [Ref. 4]. Under this definition, we can say that an antenna is a coupling device that connects the transmitting or receiving device to the medium. An antenna may be designed for only transmitting or only receiving or both transmitting and receiving purposes [Ref. 4].

An antenna can be any conductive structure that can carry an electrical current. If it carries a time varying electrical current, it will radiate an electromagnetic wave, maybe not efficiently or in a desirable manner but it will radiate. Usually one designs a structure to radiate efficiently with certain desired characteristics. If one is not careful, other things may radiate also including the transmission line, the power supply line, nearby structures or even a person touching the equipment to which the antenna is connected [Ref. 5].

By providing matching of antenna impedance to its connecting transmission line, the antenna can transfer power efficiently. The transmission line should transfer all of its power to the antenna and not radiate energy itself. As a result, the impedance of the transmission line should be matched to impedance of the antenna. It is normally desired that an antenna radiate in a specified direction or directions. This is achieved by designing it to have the proper radiation pattern. The antenna polarization is also an important design consideration. For MAV applications the antenna weight, size, and

installation location are limited, thereby restricting many of the design parameters normally employed to achieve the desired radiation and polarization characteristics.

B. ANTENNA IMPEDANCE

The input impedance of an antenna is the impedance presented by the antenna at its terminals. The input impedance (Z_{in}) is composed of real (R_{in}) and imaginary (X_{in}) parts. The input resistance (R_{in}) can be found from the relation $P_r = \frac{1}{2}|I|^2 R_{in}$ where P_r is the power radiated by the antenna. The input resistance of a dipole antenna is given by [Ref. 3]

$$R_{in,dipole} = \frac{Z_0 (k_0 dl)^2}{6\pi} = 80\pi^2 \left[\frac{dl}{\lambda} \right]^2 \quad (\text{II-1})$$

where Z_0 is the intrinsic impedance which equals $\sqrt{\mu_0/\epsilon_0}$ ($=120\pi$ Ohms), $k_0 = \omega\sqrt{\mu_0\epsilon_0}$ is the free-space wave number, dl is the length of a short dipole, λ is the wavelength, $\omega = 2\pi f$ is the angular frequency (rad s^{-1}), μ_0 is the permeability of vacuum (H m^{-1}), and ϵ_0 is the permittivity of vacuum (F m^{-1}). For a monopole antenna, the formula becomes [Ref. 3]

$$R_{in,mono} = 160\pi^2 \left[\frac{h}{\lambda} \right]^2 \quad (\text{II-2})$$

where h is the length of the monopole antenna ($h=0.5dl$). Ideally the input impedance should be a constant resistance equal to the radiation resistance in order to have maximum power transfer [Ref. 6].

The MAV telemetry antenna is basically a monopole antenna mounted on a disk. A 50-Ohm coaxial cable was used as transmission line, and the antenna designed in order to match the transmission line.

C. RADIATION PATTERN

The radiation pattern of the antenna is the relative distribution of radiated power as a function of direction in space [Ref. 6]. The radiation pattern is plotted in order to represent the received signal strength graphically for a constant transmit power. If a dipole antenna were electrically small then it would appear to be a point source and would radiate with a pattern that looks like the cross section of a donut. The radiation pattern of a dipole and the coordinate system are shown in Figure 2.1.

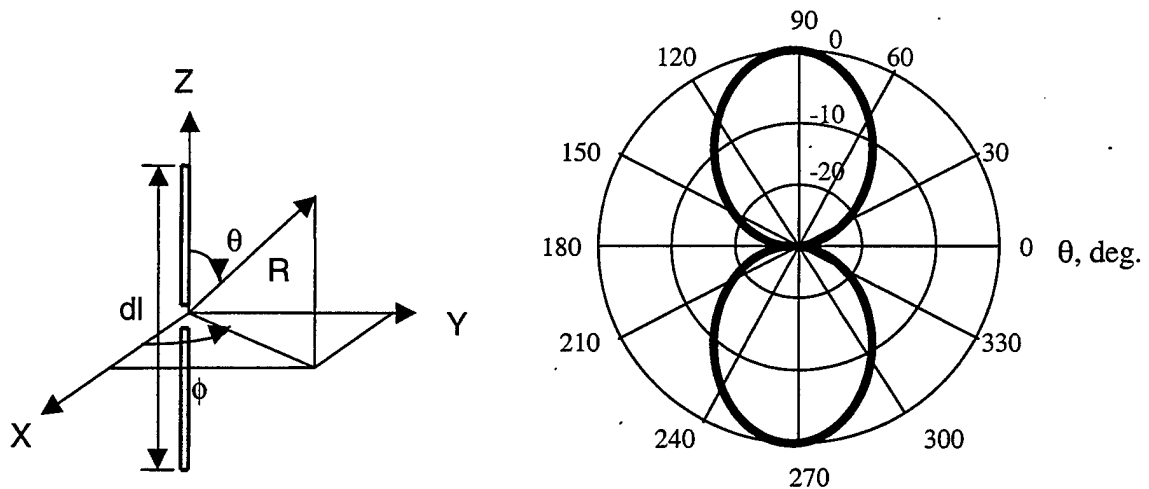


Figure 2.1 Coordinate system and radiation pattern of a typical short dipole.

Another parameter which is frequently used is the *half-power beamwidth*, which is defined as the angular width between points at which the radiated power per unit area is one-half of the maximum.

The radiation pattern can be considered as the first design parameter for the antennas. For this study, the baseline telemetry antenna is a monopole and candidate GPS antennas include crossed-dipoles, tripole, conical spiral, helix, slotted-ring, and microstrip antenna types. The performance goals of the antennas were achieved through an iterative design process using computer simulations. For the telemetry antenna, the goal was an ideal dipole antenna radiation pattern. For the GPS antenna, the radiation pattern should provide a nearly hemispherical pattern with maximum gain above the aircraft.

D. POLARIZATION

All transverse electromagnetic (TEM) waves traveling in free space have an electric field component, \vec{E} , and a magnetic field component, \vec{H} , which are mutually perpendicular to each other and to the direction of propagation. The orientation of the \vec{E} vector is used to define the polarization of the wave: if \vec{E} is orientated vertically with respect to the ground, the wave is said to be vertically polarized. Conversely, if \vec{E} is parallel to the ground, the wave is said to be horizontally polarized. Sometimes the E field vector rotates with time and it is said to be circularly or elliptically polarized. Polarization of the wave radiating from an antenna is an important concept when one is concerned with the coupling between two antennas or the propagation of a radio wave.

A closely related parameter is the impedance of a wave; this is the ratio of $Z_0 = \frac{|\vec{E}|}{|\vec{H}|}$ and for free space it is approximately 377 Ohms. If a propagating radio wave encounters a medium of a different impedance, part of the wave is reflected, much like the reflections at a discontinuity in a transmission line. The remaining energy of the

wave that passes through the discontinuity is refracted, just like the distortion one sees as a light beam passes through water. The reflection and refraction properties often depend upon the polarization of the EM wave [Ref. 5].

Polarization is one of the most important issues when designing the GPS antenna for the MAV. The GPS satellites transmit right-handed circularly polarized signals, and this is the reason for the right-handed circular polarization requirement for the GPS receiving antennas.

E. DIRECTIVITY AND GAIN

Not all antennas radiate uniformly in all directions. The variation of the intensity with direction in space is described by the *directivity* function

$$D(\theta, \phi) = \frac{dP_r/d\Omega}{P_r/4\pi} \quad (\text{II-3})$$

where $dP_r/d\Omega$ is the intensity of the radiation, which is expressed in terms of the power radiated (P_r) per unit solid angle (Ω). The angle θ is measured from the z axis, and ϕ is measured from the x axis (or x - z plane) [Ref. 3]. The ratio $P_r/4\pi$ is the average power radiated per unit solid angle. The directive gain also can be written as

$$D(\theta, \phi) = D_0 |F(\theta, \phi)|^2 \quad (\text{II-4})$$

where $|F(\theta, \phi)|^2$ is a function that has a maximum value of unity. Therefore, the maximum of the directive gain is the directivity (simply denoted D_0). For the dipole antenna the total radiated power is defined as [Ref. 3]

$$P_r = \frac{I^* Z_0 (dl)^2 k_0^2}{32\pi^2} \int_0^{2\pi} \int_0^\pi \sin^2 \theta \sin \theta d\theta d\theta \quad (\text{II-5})$$

or

$$P_r = \frac{I^* Z_0 (dl)^2}{12\pi} \quad (\text{II-6})$$

and

$$\frac{dP_r}{d\Omega} = \frac{I^* Z_0 (dl)^2 k_0^2 \sin^2 \theta}{32\pi^2} \quad (\text{II-7})$$

where I is the feed current and “*” denotes a complex conjugate. Substituting Equation (II-6) and Equation (II-7) in Equation (II-3) gives

$$D(\theta, \phi) = 1.5 \sin^2 \theta. \quad (\text{II-8})$$

From Equation (II-8), the maximum directivity D_0 is 1.5 and occurs at the angle $\theta = \pi/2$.

The gain of an antenna is defined similar to the directivity, except that the total input power to the antenna rather than the total radiated power is used as the reference.

Therefore the gain of an antenna may be defined as follows [Ref. 7]

$$G(\theta, \phi) = \frac{dP_r/d\Omega}{P_{in}/4\pi} \quad (\text{II-9})$$

or

$$G(\theta, \phi) = 4\pi \frac{dP_r/d\Omega}{P_{in}} = \eta D(\theta, \phi) \quad (\text{II-10})$$

and

$$P_r = \eta P_{in} \quad (\text{II-11})$$

where P_{in} is the input power, and η is the radiation efficiency.

Since the monopole voltage across the terminals is half that of the dipole, the total power of the monopole is half that of the dipole [Ref. 8]. Equivalently, the beam solid angle of a monopole directivity can be defined as [Ref. 3]

$$D_{mono} = \frac{4\pi}{\Omega_{A,mono}} = \frac{4\pi}{\frac{1}{2}\Omega_{A,dipole}} \quad (II-12)$$

which gives

$$D_{mono} = 2D_{dipole} . \quad (II-13)$$

F. VOLTAGE STANDING WAVE RATIO (VSWR)

The antenna is the terminating load for the transmission line that feeds it. If the antenna impedance is $Z_L (=Z_{in})$ and the transmission line characteristic impedance is Z_C , the load reflection coefficient Γ_L is given by

$$\Gamma_L = \frac{Z_L - Z_C}{Z_L + Z_C} . \quad (II-14)$$

The voltage standing wave ratio (VSWR) is defined as the ratio of the maximum voltage to the minimum voltage on the line

$$VSWR = \frac{V_{max}}{V_{min}} = \frac{|V^+| + |V^-|}{|V^+| - |V^-|} = \frac{1 + |\Gamma_L|}{1 - |\Gamma_L|} . \quad (II-15)$$

For most applications, the impedance match is usually considered acceptable if the VSWR is less than 1.5 [Ref. 6]. Given that Z_C is known and fixed, the VSWR specification sets the range of acceptable values for Z_{in} .

For the telemetry antenna, NEC-Win computed a VSWR of 1.093 when the monopole length was 0.25λ . After building the antenna, the measured VSWR on a

network analyzer was 1.15. According to these values of *VSWR*, the telemetry antenna can be considered as “well-matched.”

III. COMPUTER CODE DESCRIPTION

The electromagnetics simulation code NEC-Win Professional (NEC-Win v1.1a) of Nittany Scientific Inc. was used for designing the GPS and telemetry antennas for the MAV. A brief description of this simulation code is presented in this chapter.

NEC-Win is an intuitive program that helps antenna designers quickly and effectively design and analyze antennas. The calculations performed by NEC-Win are based on a method of moments (MM) solution of the E -field integral equation ($EFIE$). The method of moments reduces the $EFIE$ to system of simultaneous linear algebraic equations. Using standard matrix methods, it is possible to solve for the unknown current. Once the current is known, it is a fairly straightforward procedure to determine the radiation pattern and impedance. NEC-Win computes the currents (I) that flow on a wire mesh that approximates the surface. The wire mesh approximation is accurate if the mesh dimensions are small relative to the wavelength. This approach allows some reduction in the computational load because the thin wire approximation can be used. For thin wires, the component of current directed around the circumference of the wire is negligible [Ref. 3].

For NEC-Win, the number of segments in the wire mesh determines the matrix size. Some additional unknowns are required to model the current behavior at junctions because Kirchhoff's current law must be satisfied. NEC-Win uses the powerful Numerical Electromagnetics Code (NEC) as a core for antenna analysis [Ref. 9]. Thin wires are used to create the antenna model. For that reason the structures are restricted to perfect electric conductors. Each wire has a tag and is divided into an arbitrary number of

segments. Because of the limited amount of computer memory the designers who prefer to use NEC-Win should consider that the number of wires and the number of segments are limited. For example, the computer used to design the GPS and telemetry antennas has 256 MB of memory (RAM). The operating system uses about 6 MB leaving NEC-Win a maximum of 250 MB of RAM. By means of a formula given by [Ref. 9], the limitation on the number of segments can be calculated before or during the antenna design from

$$N_{MAX} = \sqrt{\frac{RAM}{16}} \quad (III-1)$$

Using Equation (III-1) the maximum number of segments can be found as 3952. Actually the maximum number of segments used for the MAV is 1423 which is far below the maximum limit.

The segment lengths should not exceed 0.1 wavelength. The maximum wire radius is also dependent on wavelength, and it should follow the rule [Ref. 9]

$$\frac{(2\pi a)}{\lambda} \ll 1 \quad (III-2)$$

where a is the wire radius and λ is the wavelength.

NEC-Win provides many options for output such as *VSWR* vs. frequency, power gains vs. angle, radiated E -fields, electric field vs. angle, polarization, input impedance, currents, near fields, and receive patterns.

IV. TELEMETRY ANTENNA

A. INTRODUCTION

The first objective of this thesis is to design, test, and build a compact and lightweight telemetry antenna for a MAV. The antenna will be used to transmit and receive video and telemetry data between the MAV and the ground station using standard FM with a 2.45 GHz carrier. A dipole type of pattern is sufficient for maintaining the link considering that the MAV flies at relatively low altitudes and at distances up to 10 km [Ref. 10].

A previous feasibility study regarding the telemetry antenna for a MAV [Ref. 3] presented several antenna configurations which were simulated using computer codes NEC-Win and PATCH for the frequency of 1 GHz. They included a monopole on a disk, a top-loaded monopole on a cylindrical cap, and a circular loop over a disk. All of the antennas contained a conducting disk, which represented the bottom surface of the MAV body. Based on the computer simulations of those configurations, Suksong recommended that a monopole on a cylindrical end cap be selected as the design for the telemetry antenna. That configuration had the lowest *VSWR* at 1.0113 GHz (1.02:1) and an input impedance of $Z_{in}=50.7+j0.008$ Ohms at 1 GHz [Ref. 3]. Similar performance can be achieved at 2.45 GHz by simply frequency scaling the monopole geometry.

Building on the results of the previous study, the telemetry antenna was designed as a monopole on a cylindrical end cap. The antenna was designed and simulated by using NEC-Win. After optimizing the design on the computer, the antenna was built in the microwave laboratory. The data is presented in following sections.

B. COMPUTER SIMULATION

The telemetry antenna was designed to have a length of one quarter of wavelength ($\lambda/4$). That means the length of the antenna was 3.061 cm (1.205 in) for the selected carrier frequency of 2.45 GHz. The end cap height was selected as 2.54 cm (1 in) in order to improve the antenna's match with the transmission line, which has an impedance of 50 Ohms. The dimensions of the telemetry antenna model are shown in Figure 4.1. The monopole points toward the ground when the UAV is flying straight and level.

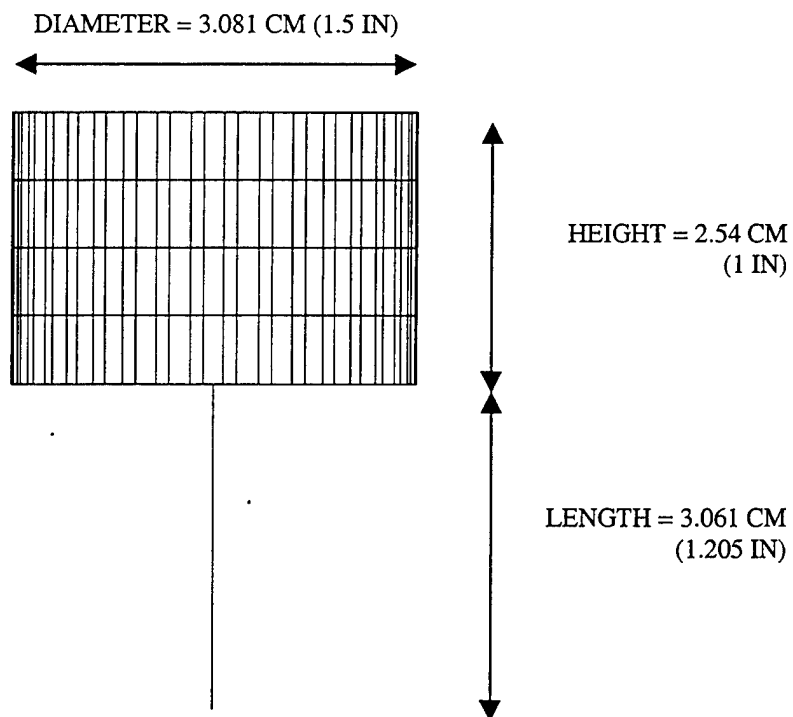


Figure 4.1 The NEC-Win design model of the telemetry antenna (side view).

The NEC-Win input file for a monopole telem1.nec is shown in APPENDIX A. The VSWR values for the telemetry antenna resulting from the NEC-Win simulation are shown in Table 4.1.

Table 4.1. VSWR values from NEC-Win simulation of the telemetry antenna.

FREQUENCY (MHz)	VSWR
2440	1.107
2450	1.093
2460	1.088

The input impedance values for the telemetry antenna that were calculated by the simulation are shown in Table 4.2.

Table 4.2. Input impedance values from NEC-Win simulation of the telemetry antenna.

FREQUENCY (MHz)	INPUT IMPEDANCE (Ohms)
2440	45.3197-j1.29417
2450	45.7086-j1.30911
2460	46.0987+j1.03273

The radiation pattern of the telemetry antenna was plotted using a MATLAB program (telem1.m) by importing the NEC-Win simulation output file values for the electric field of the telemetry antenna. The radiation pattern is shown in Figure 4.2. The coordinate system is defined so that the z axis is coincident with the MAV body axis. Therefore 0° is up, 180° is down, and $\pm 90^\circ$ the horizon when the vehicle is flying straight and level.

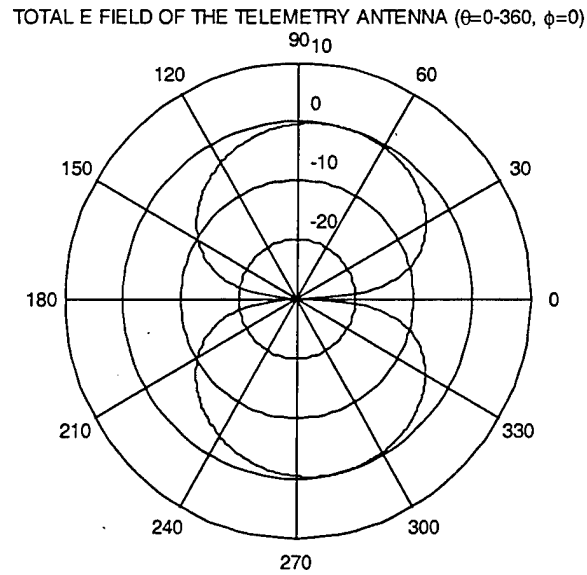


Figure 4.2 The radiation pattern of the telemetry antenna (the reference level 0 dB is 1.87 dBi).

A NEC-Win model of the telemetry antenna mounted under the bottom of the MAV (telem2.nec) is shown in Figure 4.3. The radiation pattern is presented in Figure 4.4. The effect of the body is to slightly reduce the gain in the upper hemisphere and to increase it in the lower hemisphere.

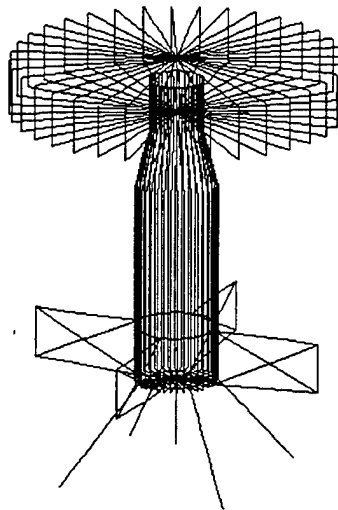


Figure 4.3 NEC-Win model of MAV with the telemetry antenna.

TOTAL E FIELD OF THE TELEMETRY ANTENNA ($\theta=0-360$, $\phi=0$)

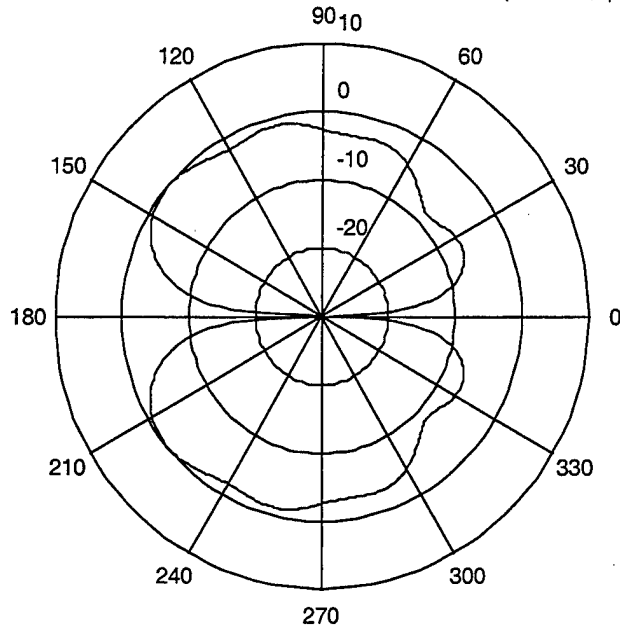


Figure 4.4 Radiation pattern of the telemetry antenna with the whole structure (the reference level 0 dB is 2.95 dBi).

C. PROTOTYPE OF THE TELEMETRY ANTENNA

After obtaining the satisfactory *VSWR* and input impedance values from NEC-Win, the telemetry antenna was built in the NPS Microwave Laboratory. A copper cap was used for the cylindrical body of the antenna. For the transmission line, a 50-Ohm coaxial cable was installed through a hole in the copper cap and the outer conductor soldered to the bottom of the copper cap. The prototype telemetry antenna is shown in Figure 4.5.

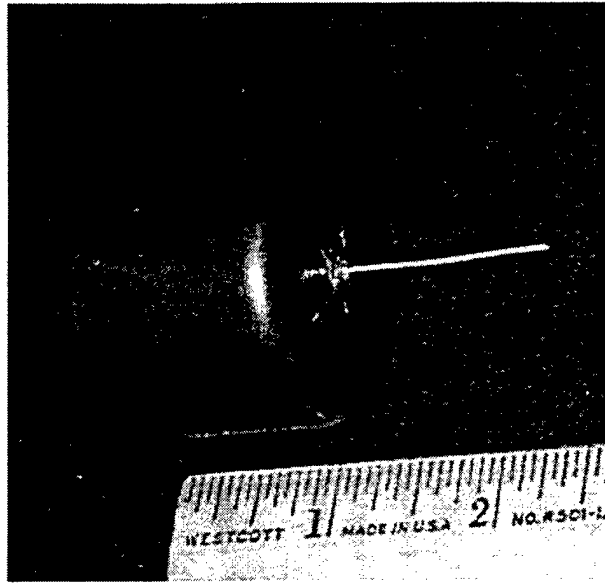


Figure 4.5 The picture of the prototype telemetry antenna.

The telemetry antenna was tested by using a HP Vector Network Analyzer. The VSWR values are shown in Table 4.3. The measured impedance values are listed in Table 4.4.

Table 4.3. The VSWR values of antenna using HP Analyzer.

FREQUENCY (MHz)	VSWR
2440.00-2451.20	1.15
2452.80-2454.40	1.16
2456.00-2457.60	1.17
2459.20	1.18

Table 4.4. The input impedance values of the antenna using HP Analyzer.

FREQUENCY (MHz)	INPUT IMPEDANCE (Ohms)
2440.00	41.49-j5.49
2441.60	41.32-j5.14
2443.20	41.19-j4.19
2444.80	41.10-j4.65
2446.40	41.06-j4.44
2448.00	40.94-j4.30
2449.60	40.81-j4.12
2451.20	40.63-j3.96
2452.80	40.49-j3.86
2454.40	40.27-j3.78
2456.00	40.00-j3.68
2457.60	39.71-j3.50
2459.20	39.38-j3.29

Figures 4.6 and 4.7 compare the measured and predicted VSWR and input impedance values.

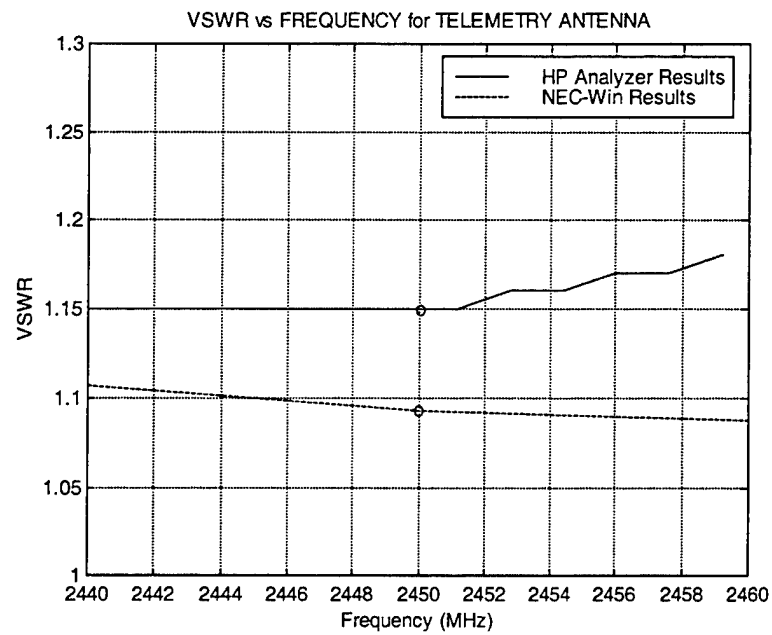


Figure 4.6 The VSWR values of NEC-Win model and the prototype of the telemetry antenna.

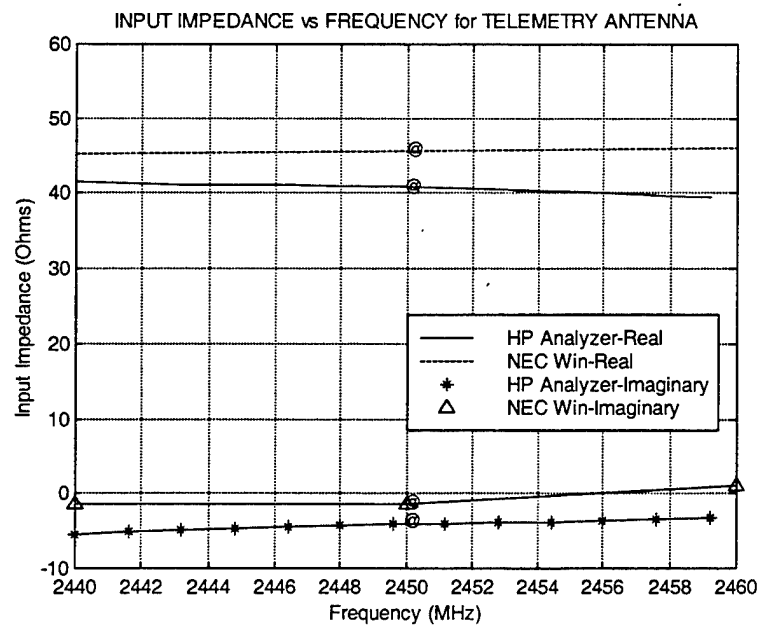


Figure 4.7 The input impedance values of NEC-Win model and the prototype of the telemetry antenna.

In conclusion, the measured radiation pattern, input antenna impedance, and VSWR of the prototype telemetry antenna were very close to those of the NEC-Win designed model. The telemetry antenna for the MAV was built and tested in accordance with the requirements. Although the weight of the prototype antenna is still considerably beyond the ideal weight, a much lighter model one can be made by depositing a thin metallic film on top of the graphite MAV body.

THIS PAGE INTENTIONALLY LEFT BLANK

V. GPS ANTENNA

A. INTRODUCTION

The GPS antenna will be used to receive signals from GPS satellites [Ref. 10]. The GPS satellites transmit right-handed circularly polarized (RHCP) signals. The main reason that the antenna must be right-handed circularly polarized is to minimize polarization mismatch. In addition, there will be high rejection of cross-polarized reflected signals. This is because RHCP waves have the property of becoming left-handed circularly polarized (LHCP) after reflection from the ground. The radiation pattern of the receiving antenna is also very important in the design specifications. While hemispherical coverage is required to receive signals from all satellites, a very sharp slope is also desirable near the horizon to minimize the effect of the multipath signals. These two requirements appear to be mutually exclusive and, therefore, impose very restrictive conditions on the antenna design. Furthermore, as the signal received by the antenna is very weak, the impedance matching is a very important aspect of the design [Ref. 11]. In many applications the gain of a passive antenna is not sufficient to maintain the minimum number of satellite links. In these cases, active antennas can be used. Embedded low noise amplifiers (LNAs) effectively increase the gain by 10-20 dB. Typical antenna requirements are listed Table 5.1.

When considering a GPS antenna design for a MAV, the antenna must be very small and lightweight in order to maximize the MAV performance. The GPS antenna should have a clear hemispherical view above the aircraft in order to have an unobstructed view of satellites when it is in straight and level flight.

Table 5.1. Typical requirements for a fixed reception pattern GPS antenna [Ref. 12].

PARAMETER	RANGE OF VALUES
Gain	-2.5 dBi from 10 degrees above the horizon -7.5 dBi on the horizon
Frequencies	L1=1575.42 MHz, $\lambda=0.19$ m L2=1227.6 MHz, $\lambda=0.244$ m
Polarization	Right hand circular
Axial ratio	6 dB
VSWR	2:1
Maximum power density (Burnout protection)	69 kW/m ² for 10 μ s 348 W/m ² CW
Out of band rejection	35 dB at 1625 MHz
Preamplifier gain	23 dB
Noise figure	4 dB

In this study, five candidate GPS antennas are presented for a MAV: (1) microstrip patch, (2) helix, (3) conical spiral, (4) tripole, (5) crossed-dipole, and (6) slotted-ring antennas. The advantages and disadvantages of these antennas will be discussed in the following section. Figure 5.1 shows how each antenna concept would be implemented.

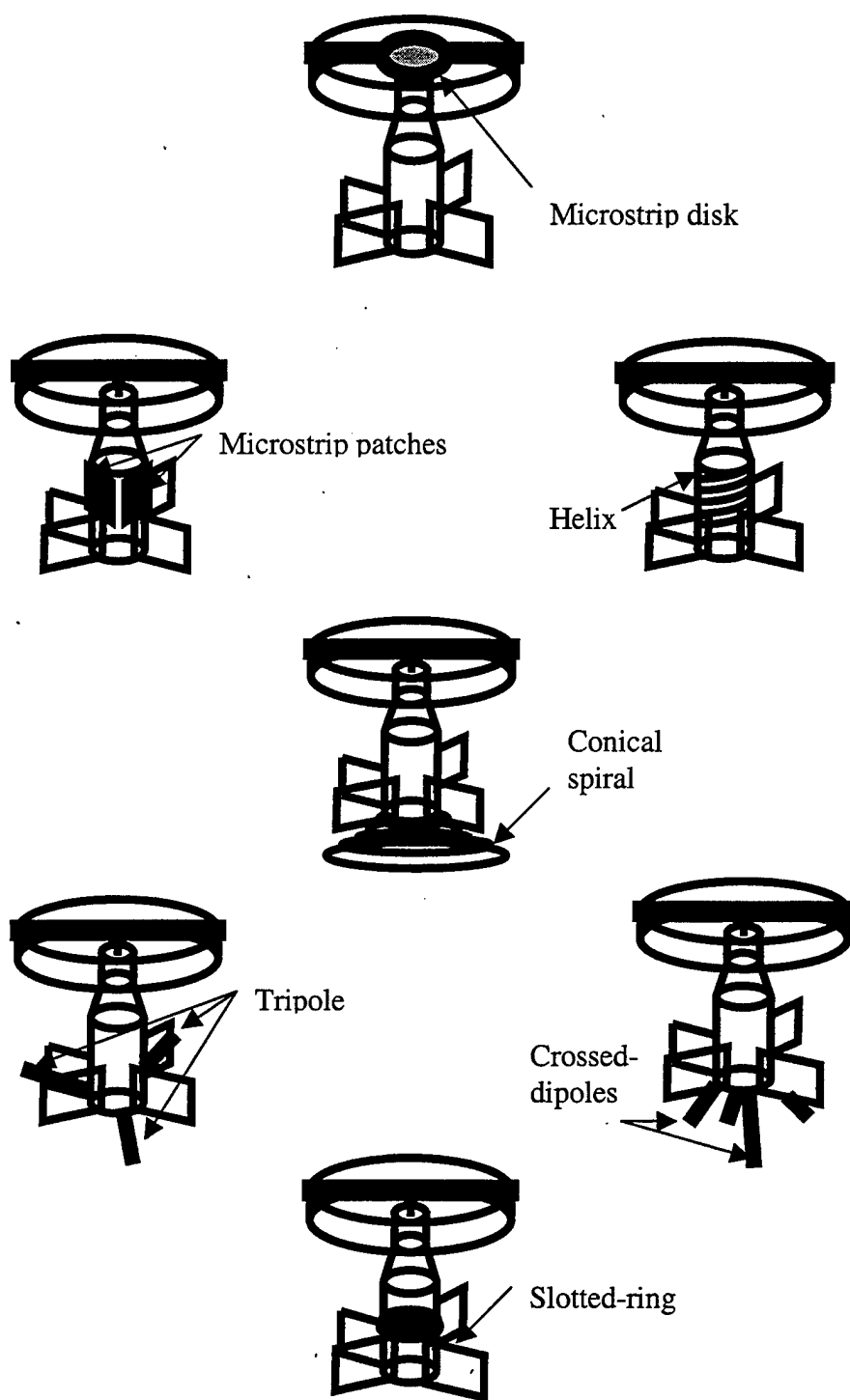


Figure 5.1 MAV with GPS antenna configurations depicted.

B. MICROSTRIP PATCH ANTENNA

The de facto standard for small GPS antennas is a microstrip patch, or simply “patch” antenna. Patch antennas consist of a thin rectangular substrate of dielectric material, like ceramic, plated with smaller area of metal (see Figure 5.2). Patch antennas require a ground plane. In theory, the ideal ground plane for a patch antenna is of infinite size. Practically speaking, the ground plane must be significantly larger than the patch itself. Performance of the antenna is directly correlated to the size of the antenna and relative size of ground plane. The orientation of a patch antenna also affects its performance. For the best performance, patch antennas should be oriented parallel to the ground [Ref. 13].

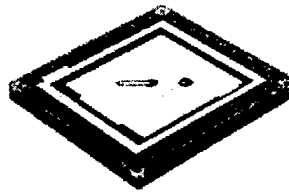


Figure 5.2 Typical microstrip patch antenna.

Patch antennas present radiation patterns with a broad lobe over a hemisphere. This provides the required hemispherical coverage for GPS applications. Relative low cost, low profile, and lightweight are additional features of patch antennas. These features make patch antennas an attractive design possibility. Patch antennas, however, are inherently narrowband [Ref. 13]. The frequency of resonance is determined by the dimensions of the rectangular patch and the thickness and type of dielectric substrate [Ref. 14].

Circular polarization can be obtained using a proper feed arrangement and an adequate width-to-length ratio [Ref. 15]. Circular polarization can be generated from

aperture-coupled elements by using off-center coupling apertures [Ref. 16] or with crossed slots [Refs. 17-18]. In both cases, two orthogonal linearly polarized modes are independently excited with equal amplitudes and a 90° phase shift, leading to good axial ratio bandwidth [Ref. 19].

Microstrip feed networks can also be used and are generally comprised of 90° hybrids such as branch line or ratrace couplers, or T-splitters in order to obtain right-hand circular polarization and to provide a matched input to the antenna.

Most commercially available off-the-shelf GPS antennas are microstrip patches with an integrated preamp. Typical diameters are on the order of 1.5 to 3 inches, but they can be made smaller. A patch would have to be placed on the top of the rotor hub, which would block air flow, change the aircraft CG (center of gravity), and require a long length of cable to reach a receiver located in the body [Ref. 10]. Alternatively two-side looking patches could be mounted on opposite sides of the body (see Figure 5.1). The measured radiation pattern of a single patch is shown in Figure 5.3 [Ref. 20].

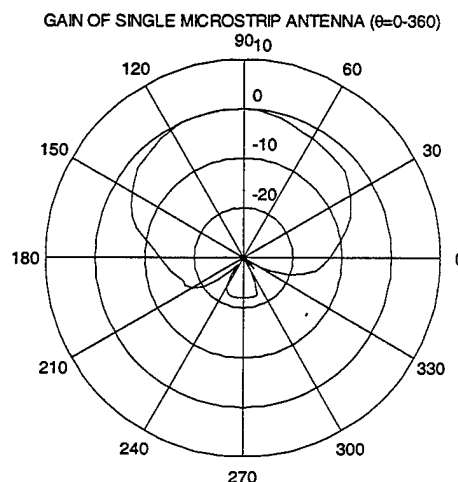


Figure 5.3 Radiation pattern of a single side mounted patch antenna (the maximum gain is 5 dBi).

The combined radiation pattern of two side-mounted patches provides sufficient antenna coverage as shown in Figure 5.4.

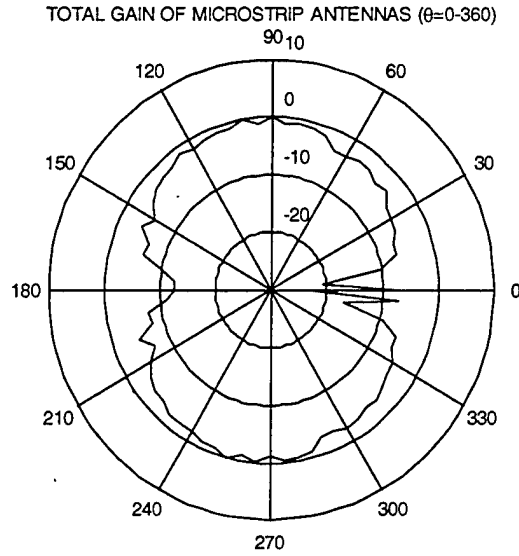


Figure 5.4 Radiation pattern of two patch side-mounted antennas (the maximum gain is 5 dBi).

C. HELIX ANTENNA

Helix antennas present circular polarization, a broad frequency band, and are relatively insensitive to mutual coupling effects. Because of these desirable features, these antennas are suitable for use in GPS applications [Ref. 11].

A helix is described by the following parameters [Ref. 10]:

- | | |
|--|---|
| D = diameter of helix (center to center), | A = axial length = nS , |
| C = circumference of helix = πD , | S = spacing between turns (center to center), |
| L = length of one turn, | n = number of turns, |
| α = pitch angle = $\arctan S/\pi D$, | d = diameter of helix conductor. |

Conventional helices operate with air or low-dielectric cores. If the helix is assumed to be wound around the outside of the MAV body, then the diameter would have to be at

least 1.75 in (allowing for 0.125 in of insulator). This is $D = 0.23\lambda_1$ (λ_1 = wavelength at frequency L1) which corresponds to circumference of $C = 0.735\lambda_1$. Assuming that the entire bottom cylindrical portion of the body is available for winding, the length of the helix could be up to 6 inches, or $A = 0.8\lambda_1$. The longer the axial dimension, the narrower the beamwidth [Ref. 10].

For the present application, the helix must radiate in the axial mode, yet have a broad beamwidth and receive circular polarization. The condition for axial radiation is $C > \lambda$, which is just barely satisfied by the MAV body diameter. The beamwidth between first nulls (*BWFN*, or main lobe width) is approximately

$$BWFN = \frac{115^\circ}{(C/\lambda)\sqrt{NS/\lambda}} \quad (V-1)$$

when $12^\circ < \alpha < 13^\circ$. For the MAV body diameter, a pitch angle of 12 degrees, and 4 to 5 turns, the *BWFN* is an acceptable 180 degrees. Given the wavelengths of interest and the present diameter of the body, a helix is a potential candidate for the GPS antenna. An advantage of helix is that the feed circuit would be extremely simple and low loss. Helix antennas are inherently broadband. However, if the body dimensions or shape were to change, then the helix would have to be redesigned or perhaps even abandoned [Ref. 10].

By using NEC-Win, a helix antenna was designed (helix1.nec), and its radiation pattern shown Figure 5.5 was obtained. The spacing between turns is 2.54 cm (1 in), while the total length of the antenna is 12.7 cm (5 in). The radius is chosen as 1.9558 cm (0.77 in). It can be seen from the radiation pattern that the ground plane, which is the bottom of the MAV, is not large enough to prevent the downward coverage of the helix

antenna. This causes the receiving of reflected left-hand circularly polarized GPS signals, which leads to errors in the GPS position estimates.

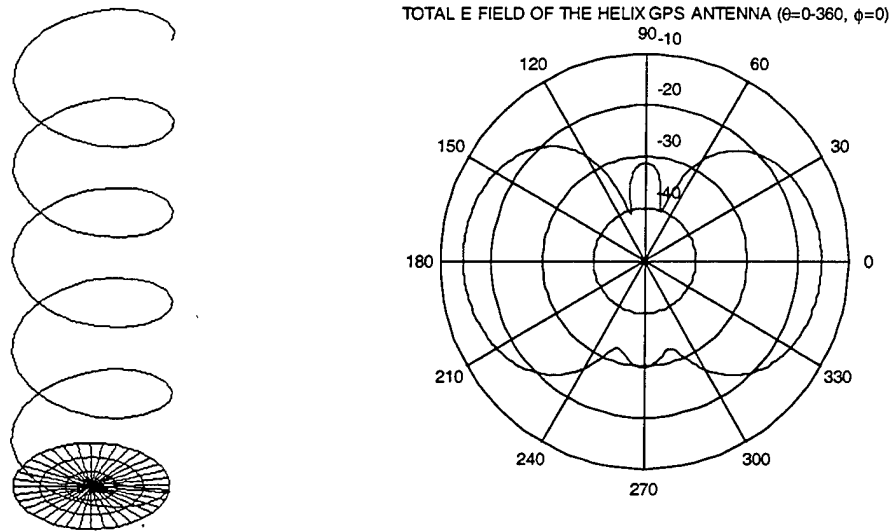


Figure 5.5 GPS helix antenna and its radiation pattern (the maximum gain is 3.26 dBi).

Another related approach is the quadrifilar helix antenna. This antenna has four helices wound around the body (Figure 5.6). These four helices are fed separately with 90 degree phase differences in order to get right-hand circular polarization. The NEC-Win simulation (helix2.nec) gave a good result for this type of antenna with regard to radiation pattern. It can be seen in Figure 5.6 that the upper lobe of the radiation pattern, which has right-hand circular polarization, is much greater than the unwanted lower lobe. The required feed arrangement is much more complicated than that for a single helix.

Both the single helix and quadrifilar helix antennas have a substantial disadvantage in terms of additional weight for the MAV. The body material of the MAV

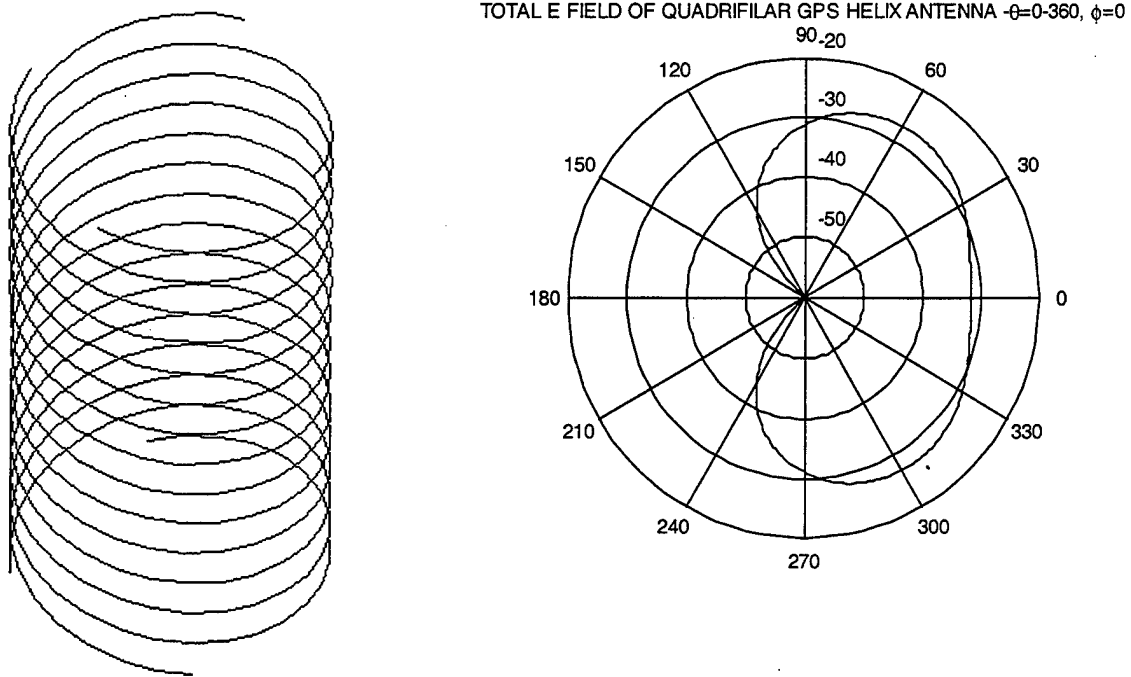


Figure 5.6 Quadrifilar helix GPS antenna and its radiation pattern (the maximum gain is 3.02 dBi).

is graphite, which is a relatively good conductor. Therefore conducting strips cannot be laid directly on the body; they would only be shorted out. Any conductor wrapped around the body would have to be spaced off of the body and insulated with dielectric. Again, this increases weight and affects the slipstream airflow [Ref. 10]. In all these cases the MAV body shell and its contents will adversely affect the gain, decreasing it overhead and increasing it on the horizon.

D. CONICAL SPIRAL ANTENNA

Another candidate antenna for the GPS application of the MAV is the conical spiral antenna. These antennas have circular polarization, broad beam, and broad frequency band. It has the advantage of one single feed point and tuning this antenna is relatively easy compared to the other candidate antenna types. The geometry of the conical antenna is shown in Figure 5.7. The spacing between turns is 4 mm (0.157 in) and the total length of the antenna is 4.4 cm (1.73 in). The smaller radius at the top is 1.905 cm (0.75 in) and the larger radius at the bottom is 6.985 cm (2.75 in). The NEC-Win input file spir.nec is shown in APPENDIX A. The radiation pattern is shown in Figure 5.8.

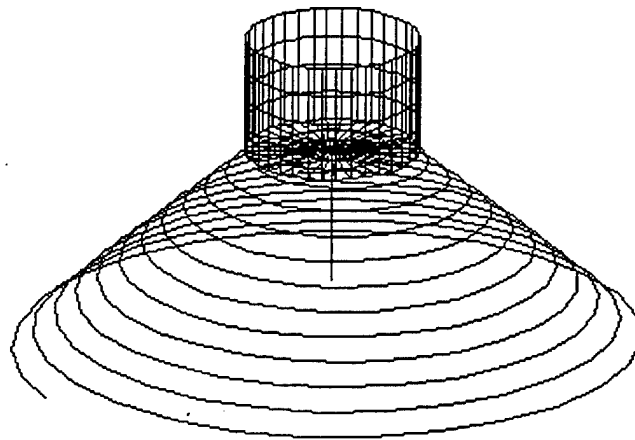


Figure 5.7 Conical spiral GPS antenna.

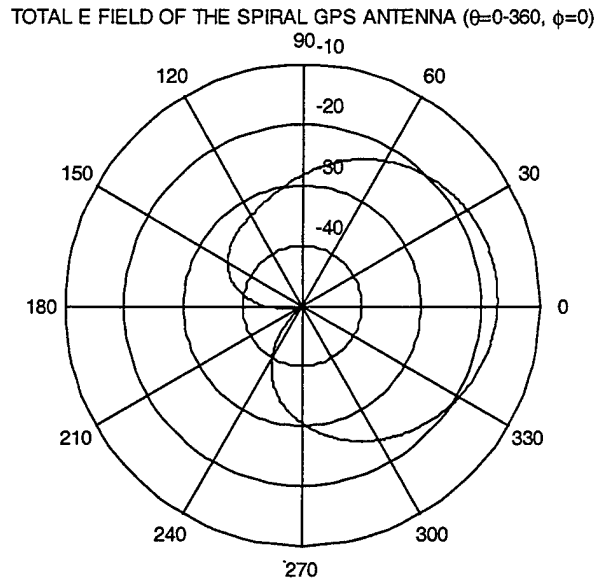


Figure 5.8 Radiation Pattern of conical spiral GPS antenna (the maximum gain is 8.08 dBi).

Although the conical spiral antenna has a very good radiation pattern in terms of coverage, polarization, and gain, it is concluded that the antenna will increase the weight and negatively affect the aerodynamic structure of the MAV.

E. TRIPOLE ANTENNA

The design trials for a very lightweight GPS antenna brought up another type of antenna for the MAV: a tripole antenna. In order to get circular polarization by using a feed with no output phase differences, three wires which have different lengths were mounted around the cylindrical body and two of them were bent backward 60 degrees. The NEC-Win model (trip.nec) is shown in Figure 5.9. The lengths of the wires are 2.381 cm (0.937 in), 3.571 cm (1.405 in), and 4.762 cm (1.875 in). In terms of the wavelength,

the difference in length is $\lambda/16$ (1.191 cm) for the GPS receiving frequency is 1.575 GHz.

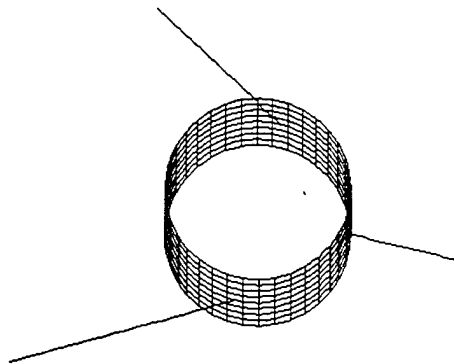


Figure 5.9 Tripole GPS antenna model.

Right hand circular polarization for the upper lobe and the left-hand circular polarization for the lower lobe were obtained, yet the unwanted lower lobe was as big as the upper lobe as shown in Figure 5.10.

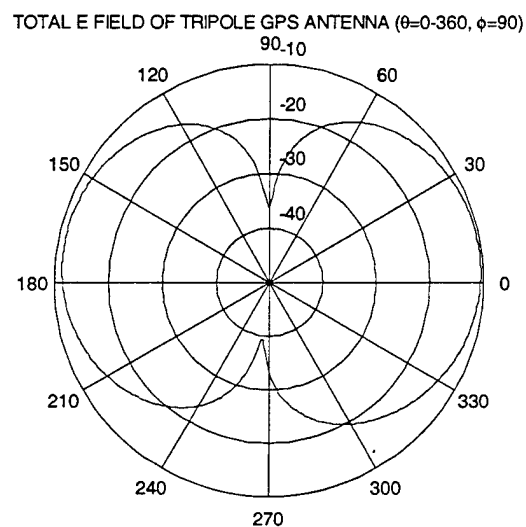


Figure 5.10 Radiation pattern of tripole GPS antenna (the maximum gain is 4.51 dBi).

By using NEC-Win simulation the *VSWR* values found for the antenna are listed in Table 5.2.

Table 5.2. *VSWR* values for the tripole antenna.

WIRE	INPUT IMPEDANCE	VSWR
1	130 Ohms	3.5177
2	210 Ohms	2.9912
3	275 Ohms	3.8494

The *VSWR* values are bigger than the typical GPS antenna requirement values (2:1) even when individual impedance transformers were used to match the different impedance values. Additionally, the desirable sharp slope near the horizon directions ($\theta = 90^\circ$ and 270°) on the radiation pattern could not be obtained. Not having a good hemispherical coverage and poor impedance matching are the main disadvantages of the tripole.

F. **CROSSED-DIPOLE ANTENNA**

In this antenna model, the landing legs of the MAV are used for the dipole arms. They “droop” at a 45 degree angle with respect to the horizontal plane. Since they are below the stabilators they do not disturb the airflow. However, the 45 degree angle does increase the polarization loss. There is a small amount of gain reduction and axial ratio degradation associated with the bent dipole arms as opposed to horizontal arms. Ideally, an array of crossed-dipoles has a hemispherical pattern with maximum gain normal to the plane containing the dipoles. However, the presence of the body and stabilators affects

the radiation pattern [Ref. 10]. The GPS antenna and MAV body were modeled using NEC-Win (gps1.nec and gps2.nec). The GPS antenna is shown in Figure 5.11.

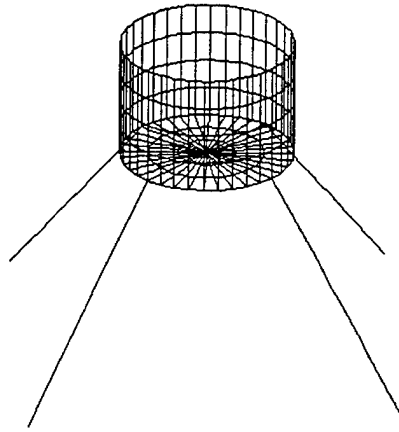


Figure 5.11 Crossed-dipole GPS antenna configuration.

When the antenna was mounted under the MAV body (see Figure 5.12) the radiation pattern in Figure 5.13 was obtained.

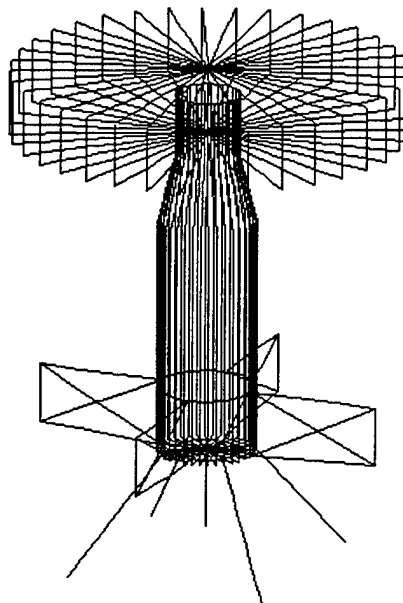


Figure 5.12 MAV with crossed-dipole and telemetry antenna at the base.

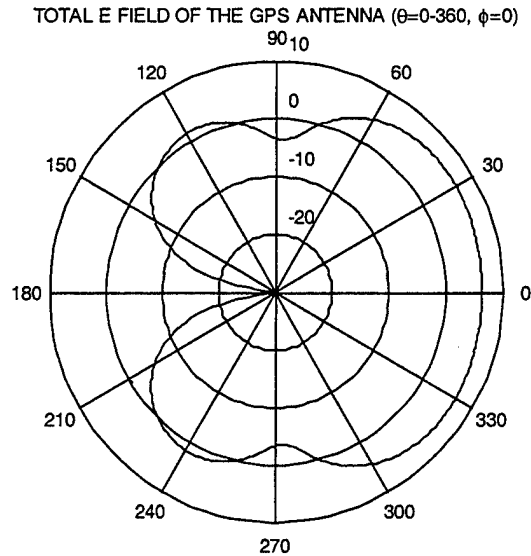


Figure 5.13 Radiation pattern of crossed-dipole GPS antenna assuming the MAV body is a perfect conductor (the maximum gain is 11.03 dBi).

Although the NEC-Win MAV model cannot include the actual MAV body material (graphite) the desirable radiation pattern for the crossed-dipole antenna was obtained. The main problem in implementing this design is miniaturizing the feed network required to provide circular polarization. Operationally, the major disadvantage of using the landing legs is the event that one of the legs severely bent or broken. A bent leg would not be catastrophic, but decreased gain would result [Ref. 10].

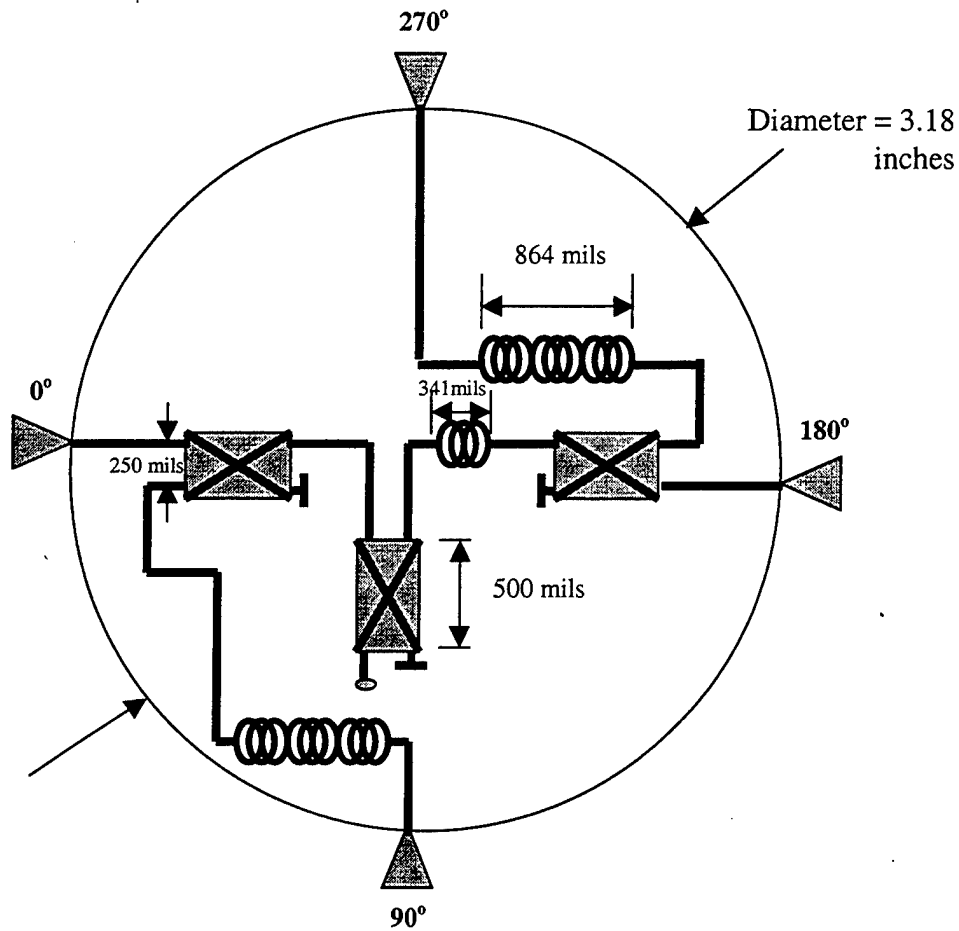


Figure 5.14 Feed network configuration for crossed-dipole antenna.

A sample feed network design was configured as shown in Figure 5.14. Relative phases of 0° , 90° , 180° , and 270° were obtained at the outputs using three 90° quadrature hybrid couplers. In order to decrease the size of the feed network disk, three surface mount inductors were used in addition to the microstrip lines. The wavelength in microstrip was calculated to be 4.59 inches for the frequency 1.575 GHz, relative permittivity 3.38, substrate thickness 20 mils, and design characteristic impedance 50 Ohms. The microstrip line width was found 46.31 mils. Two of the inductors are 0.2456 nH to provide a 227.54° phase change. Another has an inductance of 0.097 nH to obtain a 90° phase change.

G. SLOTTED-RING ANTENNA

A preliminary study of GPS antennas for a MAV [Ref. 10] presented another candidate antenna: a slotted-ring (see Figure 5.15). This antenna configuration was simulated using the computer code PATCH for the frequency of 1.575 GHz. PATCH is an electromagnetics code similar to NEC-Win, except that the conducting surface is modeled by triangular facets rather than a wire mesh [Ref. 21].

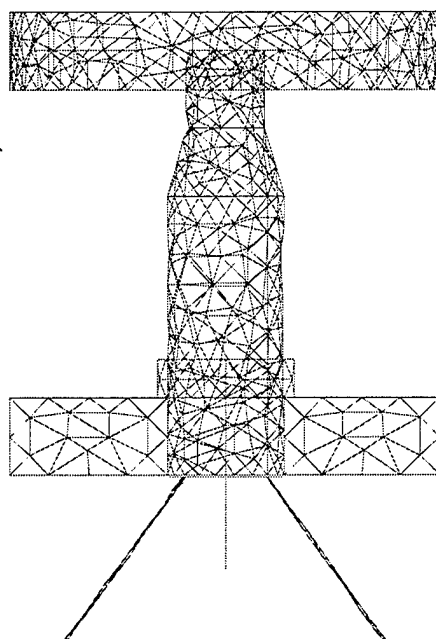


Figure 5.15 PATCH model of MAV with the slotted-ring antenna located just above the fins.

A possible feed network is shown in Figure 5.16. Microstrip transmission lines feed the slots, which are cut in the microstrip ground plane. The phase shift for circular polarization can be introduced by adjusting the open circuit lines at each element.

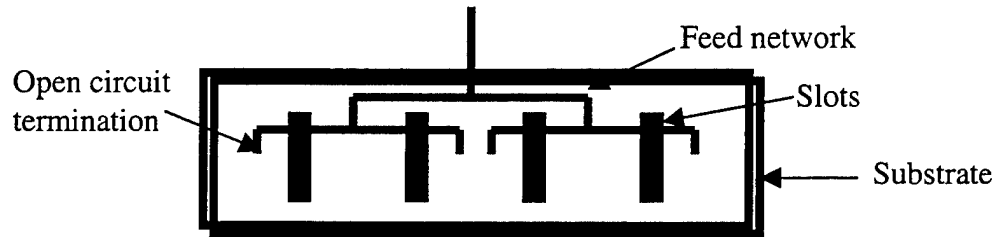


Figure 5.16 Feed network for the slotted-ring antenna.

The rectangular strip with the slots cut in it is wound around the lower cylindrical body of the MAV just above the fins. The feed lines will be on the inside of the body. The radiation pattern shown in Figure 5.17 was obtained using PATCH at 1.57 GHz [Ref. 10].

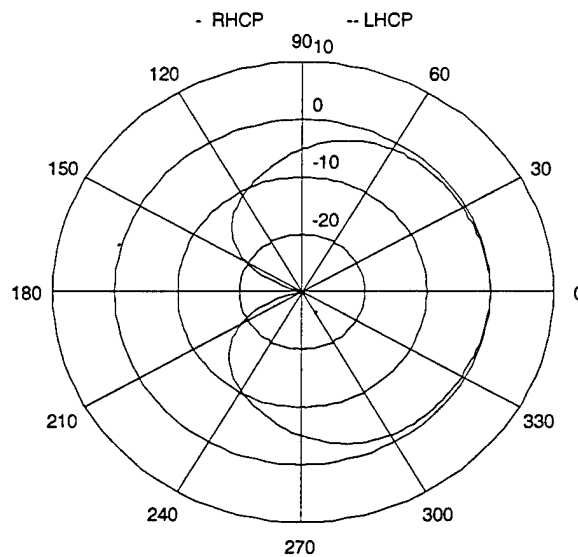


Figure 5.17 Radiation pattern of the slotted-ring antenna (The maximum gain is 4.5 dBi).

The slotted-ring antenna can be considered an optimum design in terms of getting a desirable radiation pattern employing a small feed network. The antenna does not negatively affect the aerodynamic structure of the MAV.

VI. CONCLUSION

The objective of this thesis was to design, test, and build a telemetry antenna and investigate several types of GPS antennas for a MAV. The antennas are designed with the help of a computational electromagnetics code. For design purposes, the NEC-Win electromagnetic simulation program was used to predict the radiation pattern as a function of several design parameters.

After presenting fundamental design requirements for the antennas and the NEC-Win computer code description, a monopole telemetry antenna was proposed to be mounted under the bottom of the cylindrical body of MAV. The antenna was designed as a monopole on a cylindrical end cap. After optimizing the design on the computer, the antenna was built in the NPS Microwave Laboratory. The measured *VSWR* was 1.15 and the input impedance was found to be $41.095 - j4.624$ Ohms at 2.45 GHz. The computed radiation pattern, input impedance, and *VSWR* of the prototype telemetry antenna were very close to those of the NEC-Win designed model.

Several GPS antenna types for the MAV were investigated. The radiation pattern, polarization, impedance matching, *VSWR*, and gain were presented for six candidate GPS antennas: (1) microstrip patch, (2) helix, (3), conical spiral, (4) tripole, (5) crossed-dipole, and (6) slotted-ring antennas.

The microstrip antenna was proposed as the first candidate antenna because these antennas are de facto standard for small GPS antennas. A patch would have to be placed on the top of the rotor hub, or alternatively two-side looking patches could be mounted on

opposite sides of the body. The combined radiation pattern of these two patches showed that a desirable coverage could be obtained.

Next, two helix antenna models were presented: single helix and quadrifilar helix antennas. Although the desirable radiation patterns were obtained from these antennas, both the single helix and quadrifilar helix antennas wound around the body have significant disadvantages in terms of additional weight for the MAV.

Another candidate antenna for the GPS application was the conical spiral antenna. This antenna model was quite acceptable in terms of having good axial ratio, broad beam, broad frequency band, one single feed point, and relatively easy tuning. However, it was concluded that the conical spiral antenna would increase the weight and negatively affect the aerodynamic structure of the MAV.

The tripole antenna was designed in order to have a very lightweight GPS antenna by using power splitting network with no phase differences. The radiation pattern showed that the unwanted lower lobe was unacceptably large. Additionally, the *VSWR* values were found to exceed the requirements, even if matched with higher characteristic impedance values.

For the crossed-dipole GPS antenna, the landing legs were used for the dipole arms. The computer computations showed that a desirable radiation pattern was obtained. Contingent upon the design of a very small feeding network, the crossed-dipole antenna can be a very capable GPS antenna for a MAV. At this point it is recommended that the crossed-dipole approach can be used. The landing legs can serve as the dipole arms.

A slotted-ring antenna was presented as the last candidate antenna for the MAV. This antenna configuration was taken from a GPS antenna design study for the MAV [Ref. 10]. When the GPS antenna requirements were considered, the slotted-ring provides performance similar to the crossed-dipole without the perturbing dipole arms.

For future work, the microstrip patch, crossed-dipole or slotted-ring antenna feed networks should be designed, fabricated, and installed on a MAV. Measured data should be collected to verify the various designs. This includes both *VSWR* and pattern measurements.

THIS PAGE INTENTIONALLY LEFT BLANK

APPENDIX A. NEC-WIN INPUT FILES

This appendix contains listings of all NEC-Win input files that were used to get the results posted in Chapters IV and V. These NEC-Win files are:

1. telem1.nec
2. telem2.nec
3. helix1.nec
4. helix2.nec
5. spir.nec
6. trip.nec
7. gps1.nec
8. gps2.nec

telem1.nec is designed to simulate the monopole telemetry antenna on a cylindrical end cap. The calculation frequencies are 2.40, 2.50 and 2.60 GHz.

telem2.nec is designed to simulate the monopole telemetry antenna mounted under the MAV. The calculation frequency is 2.45 GHz.

helix1.nec is designed to simulate the single helix GPS antenna mounted on a disk. The calculation frequency is 1.4 GHz.

helix2.nec is designed to simulate the quadrifilar helix GPS antenna. The calculation frequency is 1.4 GHz.

spir.nec is designed to simulate the conical spiral GPS antenna mounted on a cylindrical end cap together with the monopole telemetry antenna. The calculation frequency is 1.4 GHz.

trip.nec is designed to simulate the tripole GPS antenna. The calculation frequency is 1.575 GHz.

gps1.nec is designed to model the crossed-dipole GPS antenna mounted on a cylindrical end cap.

gps2.nec is designed to simulate the crossed-dipole GPS antenna mounted on the MAV. The calculation frequency is 1.4 GHz.

Program 1 telem1.nec

```
CM MICRO AIR VEHICLE BOTTOM STRUCTURE
CM TELEMETRY ANTENNA
CM TOGETHER WITH 1 INCH
CM CYLINDRICAL BODY
CM EXCITED WITH 2.45 GHZ
CE
GW 10,8, 0,0,0, .01905,.001666875,0, .0002286
GW 13,2, .0127,.001111125,0, .0127,-.001111125,0, .0002286
GW 14,1, .00635,.000555625,0, .00635,-.000555625,0, .0002286
GW 15,2, .01905,.001666875,0, .01905,-.001666875,0, .0002286
GW 12,3, .01905,.001666875,0, .01905,.001666875,.0254, .0002286
GW 16,2, .01905,.001666875,.0127, .01905,-.001666875,.0127, .0002286
GW 17,2, .01905,.001666875,.00635, .01905,-.001666875,.00635, .0002286
GW 18,2, .01905,.001666875,.01905, .01905,-.001666875,.01905, .0002286
GW 19,2, .01905,.001666875,.0254, .01905,-.001666875,.0254, .0002286
GM 1 35 0 0 10 0 0 0 10.19
GW 1,15, 0,0,0, 0,0,-0.030612244898, .0005
GS 0 0 1
GE 0
FR 0 3 0 0 2440 10
EX 0 1 1 00 1.0 0.0
RP 0 361 1 1000 0 0 1 1
RP 0 1 361 1000 0 0 1 1
EN
```

Program 2 telem2.nec

```
CM MICRO AIR VEHICLE TOTAL STRUCTURE
CM TELEMETRY ANTENNA IS EXCITED WITH 2.45 GHZ
CE
GW 7,13, .01352,.01352,0, .0407797, .0407797,-.04420108, .0002286
GM 0 3 0 0 90 0 0 0 7.7
```

GW 10,3, 0,0,0, .01905,.001666875,0, .0002286
 GW 12,3, .01905,.001666875,0, .01905,.001666875,0.09144, .0002286
 GW 13,2, .0127,.00111125,0, .0127,-.00111125,0, .0002286
 GW 14,1, .00635,.000555625,0, .00635,-.000555625,0, .0002286
 GW 25,1, .01905,.001666875,0.0254,.01905,-.001666875,0.0254, .0002286
 GW 30,2, .0127,.00111125,0.14224,.0127,-.0011112,0.14224, .0002286
 GW 34,3, .01905,.001666875,0.09144, .0127,.00111125,0.11684, .0002286
 GW 35,3, .0127,.00111125,0.11684, .0127,.00111125,0.14224, .0002286
 GW 37,2, .0762,.0066675,0.127, 0.0762,0.0066675,0.1524, .0002286
 GW 38,8, .0,0,0.127,0.0762,0.0066675,0.127,.0002286
 GW 39,8, 0,0,0.1524,0.0762,0.0066675,0.1524, .0002286
 GM 1 35 0 0 10 0 0 0 10.39
 GW 2,3,.01905,0,0,0.06985,0,0.00254,.0002286
 GW 3,3,0.06985,0,0.00254,0.06985,0,.0254,.0002286
 GW 4,3,0.06985,0,.0254,.01905,0,.0254,.0002286
 GW 5,3,.06985,0,0.00254,.01905,0,.0254,.0002286
 GW 6,3,.06985,0,0.0254,.01905,0,0,.0002286
 GW 102,3,-.01905,0,0,-0.06985,0,0.00254,.0002286
 GW 103,3,-0.06985,0,0.00254,-0.06985,0,.0254,.0002286
 GW 104,3,-0.06985,0,.0254,-.01905,0,.0254,.0002286
 GW 105,3,-.06985,0,0.00254,-.01905,0,.0254,.0002286
 GW 106,3,-.06985,0,0.0254,-.01905,0,0,.0002286
 GW 202,3,0,-.01905,0,0,-0.06985,.00254,.0002286
 GW 203,3,0,-.06985,.00254,0,-.06985,.0254,.0002286
 GW 204,3,0,-.06985,.0254,0,-.01905,.0254,.0002286
 GW 205,3,0,-.06985,.00254,0,-.01905,.0254,.0002286
 GW 206,3,0,-.06985,.0254,0,-.01905,0,.0002286
 GW 302,3,0,.01905,0,0,0.06985,0.00254,.0002286
 GW 303,3,0,.06985,0.00254,0,0.06985,.0254,.0002286
 GW 304,3,0,0.06985,.0254,0,.01905,.0254,.0002286
 GW 305,3,0,.06985,0.00254,0,.01905,.0254,.0002286
 GW 306,3,0,.06985,0.0254,0,.01905,0,.0002286
 GW 1,15, 0,0,0, 0,0,-0.030612244898, .0005
 GS 0 0 1
 GE 0
 FR 0 0 0 0 2450 0
 EX 0 1 1 00 1.0 0.0
 RP 0 361 1 1000 0 0 1 1
 RP 0 1 361 1000 0 0 1 1
 EN

Program 3 helix1.nec

CM MICRO AIR VEHICLE BODY STRUCTURE
 CM GPS HELIX ANTENNA EXCITED WITH
 CM 1.4 GHZ
 CE

GW 10,8, 0,0,-.002 .01905,.001666875,-.002, .0002286
 GW 13,2, .0127,.00111125,-.002, .0127,-.00111125,-.002, .0002286
 GW 14,1, .00635,.000555625,-.002, .00635,-.000555625,-.002, .0002286
 GW 15,2, .01905,.001666875,-.002, .01905,-.001666875,-.002, .0002286
 GM 1 35 0 0 10 0 0 0 10.15
 GH 1 100 .0254 -.127 .019558 .019558 .019558 .019558 .0002286
 GW 2,1, 0,0,-.002, 0,0,-.001, .0002286
 GW 3,5, 0,0,-.001,0, .019558,0, .0002286
 GS 0 0 1
 GE 0
 FR 0 0 0 0 1400 0
 EX 0 2 1 00 1.0 0.0
 RP 0 361 1 1000 0 0 1 1
 RP 0 1 361 1000 0 0 1 1
 EN

Program 4 helix2.nec

CM QUADRIFILAR GPS HELIX ANTENNA
 CM EXCITED WITH 1.4 GHZ
 CE
 GH 1 100 .0254 -.09144 .019558 .019558 0.019558 0.019558 .0002286
 GM 1 3 0 0 90 0 0 0 0
 GS 0 0 1
 GE 0
 FR 0 0 0 0 1400 0
 EX 0 1 1 00 1.0 0.0
 EX 0 2 1 00 0.0 -1.0
 EX 0 3 1 00 -1.0 0.0
 EX 0 4 1 00 0.0 1.0
 RP 0 361 1 1000 0 0 1 1
 RP 0 1 361 1000 0 0 1 1
 EN

Program 5 spir.nec

CM MICRO AIR VEHICLE BOTTOM STRUCTURE
 CM GPS HELIX ANTENNA EXCITED WITH
 CM 1.4 GHZ
 CE
 GH 1 300 .004 -.044 .01905 .01905 .06985 .06985 .0002286
 GM 0 0 180 0 0 0 0 -.001 0
 GW 10,8, 0,0,0, .01905,.001666875,0, .0002286
 GW 13,2, .0127,.00111125,0, .0127,-.00111125,0, .0002286
 GW 14,1, .00635,.000555625,0, .00635,-.000555625,0, .0002286
 GW 12,3, .01905,.001666875,0, .01905,.001666875,.0254, .0002286

GW 15,1, .01904,.001666875,0, .01904,-.001666875,0, .0002286
 GW 16,2, .01905,.001666875,.0127, .01905,-.001666875,.0127, .0002286
 GW 17,2, .01905,.001666875,.00635, .01905,-.001666875,.00635, .0002286
 GW 18,2, .01905,.001666875,.01905, .01905,-.001666875,.01905, .0002286
 GW 19,2, .01905,.001666875,.0254, .01905,-.001666875,.0254, .0002286
 GM 20 35 0 0 10 0 0 0 10.19
 GW 1,15, 0,0,0, 0,0,-0.030612244898, .0005
 GS 0 0 1
 GE 0
 FR 0 0 0 0 1400 0
 EX 0 1 1 00 1.0 0.0
 RP 0 361 1 1000 0 0 1 1
 RP 0 1 361 1000 0 0 1 1
 EN

Program 6 trip.nec

CM TRIPOLE GPS ANTENNA
 CM EXCITED WITH 1.575 GHZ
 CE
 GW 10,20, 0,0,.0127, 0, .02381,.0127, .0004
 GM 0 0 0 0 0 0 .01905 0 10.10
 GW 20,25, 0,0,.0127, -.035714,0,.0127, .00047
 GM 0 0 0 0 60 -.01905 0 0 20.20
 GW 30,30, 0,0,.0127,.047619,0,.0127, .0004
 GM 0 0 0 0 -60 .01905 0 0 30.30
 GW 63,2, .01905,.001666875,0, .01905,-.001666875,0, .00032
 GW 64,3, .01905,.001666875,0,.01905,.001666875,.0254, .00032
 GW 65,2, .01905,.001666875,.0127, .01905,-.001666875,.0127, .00032
 GW 66,2, .01905,.001666875,.00635, .01905,-.001666875,.00635, .00032
 GW 67,2, .01905,.001666875,.01905, .01905,-.001666875,.01905, .00032
 GW 68,2, .01905,.001666875,.0254, .01905,-.001666875,.0254, .00032
 GW 71,2, .01905,.001666875,.003175, .01905,-.001666875,.003175, .00032
 GW 72,2, .01905,.001666875,.009525, .01905,-.001666875,.009525, .00032
 GW 73,2, .01905,.001666875,.015875, .01905,-.001666875,.015875, .00032
 GW 74,2, .01905,.001666875,.022225, .01905,-.001666875,.022225, .00032
 GM 1 35 0 0 10 0 0 0 63.74
 GS 0 0 1
 GE 0
 FR 0 0 0 0 1575 0
 EX 0 10 1 00 1.0 0.0
 EX 0 20 1 00 1.0 0.0
 EX 0 30 1 00 1.0 0.0
 RP 0 361 1 1000 0 90 1 1
 RP 0 1 361 1000 90 0 1 1
 EN

Program 7 gps1.nec

CM MICRO AIR VEHICLE BOTTOM STRUCTURE
CM TOGETHER WITH TELEMETRY ANTENNA AND
CM 1 INCH CYLINDRICAL BODY
CM GPS ANTENNAS ARE EXCITED
CM WITH FREQUENCY OF 1.4 GHZ
CE
GW 7,13, .01352,.01352,0, .0407797, .0407797,-.04420108, .0002286
GM 0 3 0 0 90 0 0 0 7.7
GW 10,8, 0,0,0, .01905,.001666875,0, .0002286
GW 13,2, .0127,.00111125,0, .0127,-.00111125,0, .0002286
GW 14,1, .00635,.000555625,0, .00635,-.000555625,0, .0002286
GW 12,3, .01905,.001666875,0, .01905,.001666875,.0254, .0002286
GW 15,1, .01904,.001666875,0, .01904,-.001666875,0, .0002286
GW 16,2, .01905,.001666875,.0127, .01905,-.001666875,.0127, .0002286
GW 17,2, .01905,.001666875,.00635, .01905,-.001666875,.00635, .0002286
GW 18,2, .01905,.001666875,.01905, .01905,-.001666875,.01905, .0002286
GW 19,2, .01905,.001666875,.0254, .01905,-.001666875,.0254, .0002286
GM 1 35 0 0 10 0 0 0 10.19
GW 1,15, 0,0,0, 0,0,-0.030612244898, .0005
GS 0 0 1
GE 0
FR 0 0 0 0 1400 0
EX 0 7 1 00 1.0 0.0
EX 0 7 14 00 0.0 -1.0
EX 0 7 27 00 -1.0 0.0
EX 0 7 40 00 0.0 1.0
RP 0 361 1 1000 0 0 1 1
RP 0 1 361 1000 0 0 1 1
EN

Program 8 gps2.nec

CM MICRO AIR VEHICLE TOTAL STRUCTURE
CM GPS ANTENNA IS EXCITED WITH 1.4 GHZ
CE
GW 7,13, .01352,.01352,0, .0407797, .0407797,-.04420108, .0002286
GM 0 3 0 0 90 0 0 0 7.7
GW 10,3, 0,0,0, .01905,.001666875,0, .0002286
GW 12,3, .01905,.001666875,0, .01905,.001666875,0.09144, .0002286
GW 13,2, .0127,.00111125,0, .0127,-.00111125,0, .0002286
GW 14,1, .00635,.000555625,0, .00635,-.000555625,0, .0002286
GW 25,1, .01905,.001666875,0.0254,.01905,-.001666875,0.0254, .0002286
GW 30,2, .0127,.00111125,0.14224,.0127,-.0011112,0.14224, .0002286
GW 34,3, .01905,.001666875,0.09144, .0127,.00111125,0.11684, .0002286

GW 35,3, .0127,.00111125,0.11684, .0127,.00111125,0.14224, .0002286
 GW 37,2, .0762,.0066675,0.127, 0.0762,0.0066675,0.1524, .0002286
 GW 38,8, .0,0,0.127,0.0762,0.0066675,0.127,.0002286
 GW 39,8, 0,0,0.1524,0.0762,0.0066675,0.1524, .0002286
 GM 1 35 0 0 10 0 0 0 10.39
 GW 2,3,.01905,0,0,0.06985,0,0.00254,.0002286
 GW 3,3,0.06985,0,0.00254,0.06985,0,.0254,.0002286
 GW 4,3,0.06985,0,.0254,.01905,0,.0254,.0002286
 GW 5,3,.06985,0,0.00254,.01905,0,.0254,.0002286
 GW 6,3,.06985,0,0.0254,.01905,0,0,.0002286
 GW 102,3,-.01905,0,0,-0.06985,0,0.00254,.0002286
 GW 103,3,-0.06985,0,0.00254,-0.06985,0,.0254,.0002286
 GW 104,3,-0.06985,0,.0254,-.01905,0,.0254,.0002286
 GW 105,3,-.06985,0,0.00254,-.01905,0,.0254,.0002286
 GW 106,3,-.06985,0,0.0254,-.01905,0,0,.0002286
 GW 202,3,0,-.01905,0,0,-0.06985,.00254,.0002286
 GW 203,3,0,-.06985,.00254,0,-.06985,.0254,.0002286
 GW 204,3,0,-.06985,.0254,0,-.01905,.0254,.0002286
 GW 205,3,0,-.06985,.00254,0,-.01905,.0254,.0002286
 GW 206,3,0,-.06985,.0254,0,-.01905,0,.0002286
 GW 302,3,0,.01905,0,0,0.06985,0.00254,.0002286
 GW 303,3,0,.06985,0.00254,0,0.06985,.0254,.0002286
 GW 304,3,0,0.06985,.0254,0,.01905,.0254,.0002286
 GW 305,3,0,.06985,0.00254,0,.01905,.0254,.0002286
 GW 306,3,0,.06985,0.0254,0,.01905,0,.0002286
 GW 1,15, 0,0,0, 0,0,-0.030612244898, .0005
 GS 0 0 1
 GE 0
 FR 0 0 0 0 1400 0
 EX 0 7 1 00 1.0 0.0
 EX 0 7 14 00 0.0 -1.0
 EX 0 7 27 00 -1.0 0.0
 EX 0 7 40 00 0.0 1.0
 RP 0 361 1 1000 0 0 1 1
 RP 0 1 361 1000 0 0 1 1
 EN

THIS PAGE INTENTIONALLY LEFT BLANK

APPENDIX B. MATLAB PROGRAM FILE

```
% Emin Guven
% telem1.m
% This program calculates and draws the electrical field of the telemetry antenna
% of the Micro Air Vehicle when it is excited with 2.45 GHz.

% matrix "a" consists of the NEC-Win output data file of telem1.nec
% -- ANGLES -- - POWER GAINS - --- POLARIZATION --- --- E(THETA) --- --- E(PHI) ---
% THETA PHI VERT. HOR. TOTAL AXIAL TILT SENSE MAGNITUDE PHASE MAGNITUDE PHASE
% DEGREES DEGREES DB DB DB RATIO DEG. 1-RIGHT VOLTS/M DEGREES VOLTS/M DEGREES
%
% 2-LEFT
% 0-LINEAR

a=[.00 .00 -999.99 -999.99 -999.99 .00000 .00 0 3.73356E-13 111.16 9.83270E-13 150.01
1.00 .00 -31.65 -116.02 -31.65 .00003 .00 2 2.11746E-02 -134.99 1.28100E-06 19.70
2.00 .00 -25.63 -110.00 -25.63 .00003 .00 2 4.23403E-02 -134.98 2.56095E-06 19.69
3.00 .00 -22.11 -106.48 -22.11 .00003 .00 2 6.34881E-02 -134.98 3.83879E-06 19.67
4.00 .00 -19.62 -103.99 -19.62 .00003 .00 2 8.46090E-02 -134.97 5.11348E-06 19.65
5.00 .00 -17.69 -102.07 -17.69 .00003 .00 2 1.05694E-01 -134.95 6.38397E-06 19.62
6.00 .00 -16.11 -100.50 -16.11 .00003 .00 2 1.26735E-01 -134.94 7.64922E-06 19.58
7.00 .00 -14.78 -99.17 -14.78 .00003 .00 2 1.47721E-01 -134.92 8.90821E-06 19.54
8.00 .00 -13.63 -98.03 -13.63 .00003 .00 2 1.68645E-01 -134.89 1.01599E-05 19.49
9.00 .00 -12.62 -97.03 -12.62 .00003 .00 2 1.89498E-01 -134.87 1.14033E-05 19.43
10.00 .00 -11.71 -96.13 -11.71 .00003 .00 2 2.10269E-01 -134.84 1.26375E-05 19.37
11.00 .00 -10.90 -95.33 -10.90 .00003 .00 2 2.30952E-01 -134.81 1.38613E-05 19.30
12.00 .00 -10.16 -94.60 -10.16 .00003 .00 2 2.51536E-01 -134.77 1.50740E-05 19.22
13.00 .00 -9.48 -93.94 -9.48 .00003 .00 2 2.72012E-01 -134.73 1.62744E-05 19.14
14.00 .00 -8.85 -93.33 -8.85 .00003 .00 2 2.92372E-01 -134.69 1.74618E-05 19.05
15.00 .00 -8.27 -92.76 -8.27 .00003 .00 2 3.12607E-01 -134.65 1.86352E-05 18.95
16.00 .00 -7.73 -92.24 -7.73 .00003 .00 2 3.32707E-01 -134.60 1.97937E-05 18.85
17.00 .00 -7.22 -91.75 -7.22 .00003 .00 2 3.52665E-01 -134.54 2.09364E-05 18.74
18.00 .00 -6.75 -91.30 -6.75 .00003 .00 2 3.72470E-01 -134.49 2.20626E-05 18.63
19.00 .00 -6.30 -90.87 -6.30 .00003 .00 2 3.92115E-01 -134.43 2.31713E-05 18.51
20.00 .00 -5.88 -90.47 -5.88 .00003 .00 2 4.11589E-01 -134.37 2.42619E-05 18.38
21.00 .00 -5.48 -90.09 -5.48 .00003 .00 2 4.30885E-01 -134.30 2.53336E-05 18.25
22.00 .00 -5.10 -89.74 -5.10 .00003 .00 2 4.49994E-01 -134.23 2.63856E-05 18.11
23.00 .00 -4.75 -89.41 -4.75 .00003 .00 2 4.68906E-01 -134.15 2.74172E-05 17.97
24.00 .00 -4.41 -89.09 -4.41 .00003 .00 2 4.87614E-01 -134.07 2.84278E-05 17.82
25.00 .00 -4.08 -88.80 -4.08 .00003 .00 2 5.06108E-01 -133.99 2.94167E-05 17.66
26.00 .00 -3.78 -88.52 -3.78 .00003 .00 2 5.24379E-01 -133.90 3.03833E-05 17.50
27.00 .00 -3.48 -88.25 -3.48 .00003 .00 2 5.42420E-01 -133.81 3.13271E-05 17.33
28.00 .00 -3.20 -88.00 -3.20 .00003 .00 2 5.60221E-01 -133.72 3.22475E-05 17.16
29.00 .00 -2.93 -87.76 -2.93 .00003 .00 2 5.77775E-01 -133.62 3.31440E-05 16.98
30.00 .00 -2.68 -87.53 -2.68 .00003 .00 2 5.95072E-01 -133.52 3.40160E-05 16.80
31.00 .00 -2.43 -87.32 -2.43 .00003 .00 2 6.12105E-01 -133.41 3.48633E-05 16.61
32.00 .00 -2.20 -87.12 -2.20 .00003 .00 2 6.28865E-01 -133.29 3.56853E-05 16.42
33.00 .00 -1.97 -86.93 -1.97 .00003 .00 2 6.45344E-01 -133.18 3.64817E-05 16.22
34.00 .00 -1.76 -86.75 -1.76 .00003 .00 2 6.61535E-01 -133.05 3.72521E-05 16.02
35.00 .00 -1.55 -86.57 -1.55 .00003 .00 2 6.77429E-01 -132.93 3.79962E-05 15.81
36.00 .00 -1.35 -86.41 -1.35 .00003 .00 2 6.93019E-01 -132.79 3.87138E-05 15.59
37.00 .00 -1.16 -86.26 -1.16 .00003 .00 2 7.08297E-01 -132.66 3.94046E-05 15.38
38.00 .00 -.98 -86.11 -.98 .00003 .00 2 7.23256E-01 -132.52 4.00684E-05 15.15
39.00 .00 -.81 -85.98 -.81 .00003 .00 2 7.37889E-01 -132.37 4.07050E-05 14.93
```

40.00.00	-.64	-85.85	-.64	.00003	.00 2 7.52187E-01	-132.22	4.13143E-05	14.70
41.00.00	-.48	-85.72	-.48	.00003	.00 2 7.66146E-01	-132.06	4.18962E-05	14.46
42.00.00	-.33	-85.61	-.33	.00003	.00 2 7.79756E-01	-131.90	4.24505E-05	14.22
43.00.00	-.18	-85.50	-.18	.00003	.00 2 7.93014E-01	-131.73	4.29773E-05	13.98
44.00.00	-.04	-85.40	-.04	.00003	.00 2 8.05911E-01	-131.56	4.34765E-05	13.73
45.00.00	.09	-85.31	.09	.00003	.00 2 8.18441E-01	-131.38	4.39481E-05	13.48
46.00.00	.22	-85.22	.22	.00003	.00 2 8.30600E-01	-131.19	4.43922E-05	13.23
47.00.00	.34	-85.14	.34	.00003	.00 2 8.42380E-01	-131.00	4.48088E-05	12.97
48.00.00	.46	-85.07	.46	.00003	.00 2 8.53778E-01	-130.81	4.51980E-05	12.71
49.00.00	.57	-85.00	.57	.00003	.00 2 8.64787E-01	-130.61	4.55600E-05	12.44
50.00.00	.68	-84.93	.68	.00003	.00 2 8.75403E-01	-130.40	4.58949E-05	12.17
51.00.00	.78	-84.87	.78	.00003	.00 2 8.85621E-01	-130.19	4.62029E-05	11.90
52.00.00	.87	-84.82	.87	.00003	.00 2 8.95436E-01	-129.97	4.64841E-05	11.62
53.00.00	.96	-84.77	.96	.00003	.00 2 9.04845E-01	-129.75	4.67388E-05	11.35
54.00.00	1.05	-84.73	1.05	.00003	.00 2 9.13844E-01	-129.52	4.69673E-05	11.07
55.00.00	1.13	-84.69	1.13	.00003	.00 2 9.22430E-01	-129.29	4.71698E-05	10.78
56.00.00	1.21	-84.66	1.21	.00003	.00 2 9.30598E-01	-129.04	4.73466E-05	10.50
57.00.00	1.28	-84.63	1.28	.00003	.00 2 9.38347E-01	-128.80	4.74979E-05	10.21
58.00.00	1.35	-84.61	1.35	.00003	.00 2 9.45673E-01	-128.55	4.76242E-05	9.92
59.00.00	1.41	-84.59	1.41	.00003	.00 2 9.52575E-01	-128.29	4.77258E-05	9.62
60.00.00	1.47	-84.58	1.47	.00003	.00 2 9.59050E-01	-128.03	4.78030E-05	9.33
61.00.00	1.52	-84.57	1.52	.00003	.00 2 9.65097E-01	-127.76	4.78562E-05	9.03
62.00.00	1.57	-84.56	1.57	.00003	.00 2 9.70714E-01	-127.48	4.78858E-05	8.73
63.00.00	1.62	-84.56	1.62	.00003	.00 2 9.75901E-01	-127.20	4.78921E-05	8.42
64.00.00	1.66	-84.57	1.66	.00003	.00 2 9.80656E-01	-126.92	4.78757E-05	8.12
65.00.00	1.70	-84.57	1.70	.00003	.00 2 9.84980E-01	-126.63	4.78370E-05	7.81
66.00.00	1.73	-84.58	1.73	.00003	.00 2 9.88872E-01	-126.33	4.77763E-05	7.51
67.00.00	1.76	-84.60	1.76	.00004	.00 2 9.92332E-01	-126.03	4.76941E-05	7.20
68.00.00	1.79	-84.62	1.79	.00004	.00 2 9.95362E-01	-125.72	4.75910E-05	6.88
69.00.00	1.81	-84.64	1.81	.00004	.00 2 9.97962E-01	-125.41	4.74673E-05	6.57
70.00.00	1.83	-84.67	1.83	.00004	.00 2 1.00013E+00	-125.10	4.73235E-05	6.26
71.00.00	1.85	-84.70	1.85	.00004	.00 2 1.00188E+00	-124.77	4.71601E-05	5.94
72.00.00	1.86	-84.73	1.86	.00004	.00 2 1.00320E+00	-124.45	4.69777E-05	5.62
73.00.00	1.87	-84.77	1.87	.00004	.00 2 1.00409E+00	-124.11	4.67766E-05	5.30
74.00.00	1.87	-84.81	1.87	.00004	.00 2 1.00457E+00	-123.78	4.65574E-05	4.98
75.00.00	1.87	-84.85	1.87	.00004	.00 2 1.00463E+00	-123.44	4.63206E-05	4.66
76.00.00	1.87	-84.90	1.87	.00004	.00 2 1.00427E+00	-123.09	4.60667E-05	4.34
77.00.00	1.86	-84.95	1.86	.00004	.00 2 1.00350E+00	-122.74	4.57962E-05	4.02
78.00.00	1.85	-85.01	1.85	.00004	.00 2 1.00233E+00	-122.39	4.55095E-05	3.69
79.00.00	1.84	-85.06	1.84	.00004	.00 2 1.00075E+00	-122.03	4.52073E-05	3.37
80.00.00	1.82	-85.13	1.82	.00004	.00 2 9.98771E-01	-121.66	4.48900E-05	3.04
81.00.00	1.80	-85.19	1.80	.00004	.00 2 9.96398E-01	-121.30	4.45581E-05	2.72
82.00.00	1.78	-85.26	1.78	.00004	.00 2 9.93634E-01	-120.93	4.42122E-05	2.39
83.00.00	1.75	-85.33	1.75	.00004	.00 2 9.90486E-01	-120.55	4.38527E-05	2.06
84.00.00	1.72	-85.40	1.72	.00004	.00 2 9.86958E-01	-120.17	4.34801E-05	1.73
85.00.00	1.68	-85.48	1.68	.00004	.00 2 9.83056E-01	-119.79	4.30949E-05	1.40
86.00.00	1.65	-85.56	1.65	.00004	.00 2 9.78785E-01	-119.41	4.26976E-05	1.07
87.00.00	1.60	-85.64	1.60	.00004	.00 2 9.74151E-01	-119.02	4.22888E-05	.74
88.00.00	1.56	-85.73	1.56	.00004	.00 2 9.69162E-01	-118.63	4.18689E-05	.41
89.00.00	1.51	-85.82	1.51	.00004	.00 2 9.63822E-01	-118.24	4.14384E-05	.08
90.00.00	1.46	-85.91	1.46	.00004	.00 2 9.58140E-01	-117.84	4.09978E-05	-.26
91.00.00	1.41	-86.01	1.41	.00004	.00 2 9.52121E-01	-117.44	4.05476E-05	-.59
92.00.00	1.35	-86.11	1.35	.00004	.00 2 9.45773E-01	-117.04	4.00882E-05	-.92
93.00.00	1.29	-86.21	1.29	.00004	.00 2 9.39104E-01	-116.63	3.96201E-05	-1.25
94.00.00	1.22	-86.31	1.22	.00004	.00 2 9.32120E-01	-116.23	3.91438E-05	-1.59
95.00.00	1.15	-86.42	1.15	.00004	.00 2 9.24829E-01	-115.82	3.86597E-05	-1.92

96.00.00	1.08	-86.53	1.08	.00004	.00 2 9.17240E-01	-115.41	3.81682E-05	-2.26
97.00.00	1.01	-86.65	1.01	.00004	.00 2 9.09359E-01	-115.00	3.76700E-05	-2.59
98.00.00	.93	-86.77	.93	.00004	.00 2 9.01196E-01	-114.59	3.71653E-05	-2.93
99.00.00	.85	-86.89	.85	.00004	.00 2 8.92759E-01	-114.17	3.66546E-05	-3.26
100.00.00	.76	-87.01	.76	.00004	.00 2 8.84055E-01	-113.76	3.61383E-05	-3.60
101.00.00	.67	-87.14	.67	.00004	.00 2 8.75095E-01	-113.34	3.56169E-05	-3.93
102.00.00	.58	-87.26	.58	.00004	.00 2 8.65886E-01	-112.92	3.50908E-05	-4.27
103.00.00	.49	-87.40	.49	.00004	.00 2 8.56437E-01	-112.50	3.45603E-05	-4.60
104.00.00	.39	-87.53	.39	.00004	.00 2 8.46757E-01	-112.09	3.40260E-05	-4.94
105.00.00	.28	-87.67	.28	.00004	.00 2 8.36855E-01	-111.67	3.34881E-05	-5.27
106.00.00	.18	-87.81	.18	.00004	.00 2 8.26741E-01	-111.25	3.29472E-05	-5.61
107.00.00	.07	-87.96	.07	.00004	.00 2 8.16423E-01	-110.83	3.24034E-05	-5.95
108.00.00	-.04	-88.10	-.04	.00004	.00 2 8.05911E-01	-110.40	3.18574E-05	-6.28
109.00.00	-.16	-88.25	-.16	.00004	.00 2 7.95214E-01	-109.98	3.13093E-05	-6.62
110.00.00	-.28	-88.41	-.28	.00004	.00 2 7.84342E-01	-109.56	3.07596E-05	-6.95
111.00.00	-.40	-88.57	-.40	.00004	.00 2 7.73304E-01	-109.14	3.02086E-05	-7.29
112.00.00	-.53	-88.73	-.53	.00004	.00 2 7.62109E-01	-108.72	2.96567E-05	-7.62
113.00.00	-.66	-88.89	-.66	.00004	.00 2 7.50767E-01	-108.30	2.91041E-05	-7.96
114.00.00	-.79	-89.06	-.79	.00004	.00 2 7.39287E-01	-107.89	2.85514E-05	-8.29
115.00.00	-.93	-89.23	-.93	.00004	.00 2 7.27678E-01	-107.47	2.79987E-05	-8.63
116.00.00	-1.07	-89.40	-1.07	.00004	.00 2 7.15951E-01	-107.05	2.74463E-05	-8.96
117.00.00	-1.22	-89.57	-1.22	.00004	.00 2 7.04114E-01	-106.63	2.68947E-05	-9.30
118.00.00	-1.36	-89.75	-1.36	.00004	.00 2 6.92177E-01	-106.22	2.63440E-05	-9.63
119.00.00	-1.52	-89.94	-1.52	.00004	.00 2 6.80148E-01	-105.80	2.57946E-05	-9.97
120.00.00	-1.67	-90.12	-1.67	.00004	.00 2 6.68038E-01	-105.39	2.52468E-05	-10.30
121.00.00	-1.83	-90.31	-1.83	.00004	.00 2 6.55854E-01	-104.98	2.47008E-05	-10.63
122.00.00	-2.00	-90.51	-2.00	.00004	.00 2 6.43607E-01	-104.57	2.41570E-05	-10.96
123.00.00	-2.16	-90.70	-2.16	.00004	.00 2 6.31304E-01	-104.16	2.36154E-05	-11.29
124.00.00	-2.34	-90.90	-2.34	.00004	.00 2 6.18954E-01	-103.76	2.30765E-05	-11.62
125.00.00	-2.51	-91.11	-2.51	.00004	.00 2 6.06566E-01	-103.35	2.25405E-05	-11.95
126.00.00	-2.69	-91.32	-2.69	.00004	.00 2 5.94148E-01	-102.95	2.20075E-05	-12.28
127.00.00	-2.87	-91.53	-2.87	.00004	.00 2 5.81708E-01	-102.55	2.14778E-05	-12.61
128.00.00	-3.06	-91.74	-3.06	.00004	.00 2 5.69254E-01	-102.15	2.09516E-05	-12.94
129.00.00	-3.25	-91.96	-3.25	.00004	.00 2 5.56794E-01	-101.76	2.04292E-05	-13.26
130.00.00	-3.45	-92.19	-3.45	.00004	.00 2 5.44335E-01	-101.36	1.99106E-05	-13.58
131.00.00	-3.65	-92.41	-3.65	.00004	.00 2 5.31884E-01	-100.97	1.93962E-05	-13.91
132.00.00	-3.86	-92.65	-3.86	.00004	.00 2 5.19449E-01	-100.59	1.88859E-05	-14.23
133.00.00	-4.07	-92.88	-4.07	.00004	.00 2 5.07036E-01	-100.20	1.83802E-05	-14.55
134.00.00	-4.28	-93.12	-4.28	.00004	.00 2 4.94652E-01	-99.82	1.78789E-05	-14.87
135.00.00	-4.50	-93.37	-4.50	.00004	.00 2 4.82302E-01	-99.44	1.73824E-05	-15.18
136.00.00	-4.73	-93.62	-4.73	.00004	.00 2 4.69993E-01	-99.07	1.68907E-05	-15.49
137.00.00	-4.96	-93.87	-4.96	.00004	.00 2 4.57730E-01	-98.70	1.64040E-05	-15.81
138.00.00	-5.19	-94.13	-5.19	.00004	.00 2 4.45518E-01	-98.33	1.59223E-05	-16.12
139.00.00	-5.43	-94.39	-5.43	.00004	.00 2 4.33362E-01	-97.97	1.54458E-05	-16.42
140.00.00	-5.68	-94.66	-5.68	.00004	.00 2 4.21268E-01	-97.61	1.49745E-05	-16.73
141.00.00	-5.93	-94.94	-5.93	.00003	.00 2 4.09238E-01	-97.26	1.45086E-05	-17.03
142.00.00	-6.19	-95.22	-6.19	.00003	.00 2 3.97278E-01	-96.91	1.40480E-05	-17.33
143.00.00	-6.45	-95.50	-6.45	.00003	.00 2 3.85390E-01	-96.56	1.35928E-05	-17.62
144.00.00	-6.72	-95.79	-6.72	.00003	.00 2 3.73578E-01	-96.22	1.31431E-05	-17.91
145.00.00	-7.00	-96.09	-7.00	.00003	.00 2 3.61845E-01	-95.89	1.26988E-05	-18.20
146.00.00	-7.28	-96.40	-7.28	.00003	.00 2 3.50193E-01	-95.56	1.22601E-05	-18.48
147.00.00	-7.57	-96.71	-7.57	.00003	.00 2 3.38625E-01	-95.23	1.18269E-05	-18.76
148.00.00	-7.87	-97.03	-7.87	.00003	.00 2 3.27143E-01	-94.92	1.13991E-05	-19.04
149.00.00	-8.18	-97.36	-8.18	.00003	.00 2 3.15747E-01	-94.60	1.09768E-05	-19.31
150.00.00	-8.50	-97.69	-8.50	.00003	.00 2 3.04439E-01	-94.30	1.05600E-05	-19.57
151.00.00	-8.82	-98.04	-8.82	.00003	.00 2 2.93221E-01	-94.00	1.01485E-05	-19.83

152.00.00	-9.16	-98.39	-9.16	.00003	.00	2 2.82092E-01	-93.71	9.74242E-06	-20.09
153.00.00	-9.51	-98.76	-9.51	.00003	.00	2 2.71052E-01	-93.42	9.34158E-06	-20.34
154.00.00	-9.87	-99.14	-9.87	.00003	.00	2 2.60103E-01	-93.15	8.94593E-06	-20.58
155.00.00	-10.24	-99.52	-10.24	.00003	.00	2 2.49242E-01	-92.88	8.55538E-06	-20.82
156.00.00	-10.62	-99.92	-10.62	.00003	.00	2 2.38470E-01	-92.61	8.16983E-06	-21.05
157.00.00	-11.02	-100.34	-11.02	.00003	.00	2 2.27784E-01	-92.36	7.78918E-06	-21.27
158.00.00	-11.43	-100.77	-11.43	.00003	.00	2 2.17185E-01	-92.11	7.41330E-06	-21.49
159.00.00	-11.86	-101.21	-11.86	.00003	.00	2 2.06670E-01	-91.88	7.04207E-06	-21.70
160.00.00	-12.31	-101.68	-12.31	.00003	.00	2 1.96237E-01	-91.65	6.67534E-06	-21.90
161.00.00	-12.78	-102.16	-12.78	.00003	.00	2 1.85885E-01	-91.43	6.31296E-06	-22.10
162.00.00	-13.28	-102.67	-13.28	.00003	.00	2 1.75610E-01	-91.22	5.95477E-06	-22.29
163.00.00	-13.80	-103.20	-13.80	.00003	.00	2 1.65411E-01	-91.02	5.60062E-06	-22.46
164.00.00	-14.35	-103.76	-14.35	.00003	.00	2 1.55283E-01	-90.83	5.25032E-06	-22.63
165.00.00	-14.93	-104.36	-14.93	.00003	.00	2 1.45225E-01	-90.65	4.90368E-06	-22.79
166.00.00	-15.55	-104.99	-15.55	.00003	.00	2 1.35232E-01	-90.48	4.56052E-06	-22.95
167.00.00	-16.21	-105.66	-16.21	.00003	.00	2 1.25302E-01	-90.33	4.22065E-06	-23.09
168.00.00	-16.92	-106.38	-16.92	.00003	.00	2 1.15430E-01	-90.18	3.88384E-06	-23.22
169.00.00	-17.69	-107.16	-17.69	.00003	.00	2 1.05612E-01	-90.04	3.54990E-06	-23.34
170.00.00	-18.54	-108.01	-18.54	.00003	.00	2 9.58459E-02	-89.92	3.21861E-06	-23.46
171.00.00	-19.47	-108.95	-19.47	.00003	.00	2 8.61259E-02	-89.80	2.88973E-06	-23.56
172.00.00	-20.50	-109.99	-20.50	.00003	.00	2 7.64482E-02	-89.70	2.56305E-06	-23.65
173.00.00	-21.67	-111.17	-21.67	.00003	.00	2 6.68082E-02	-89.61	2.23833E-06	-23.73
174.00.00	-23.02	-112.52	-23.02	.00003	.00	2 5.72016E-02	-89.53	1.91534E-06	-23.81
175.00.00	-24.61	-114.12	-24.61	.00003	.00	2 4.76237E-02	-89.46	1.59384E-06	-23.87
176.00.00	-26.56	-116.07	-26.56	.00003	.00	2 3.80699E-02	-89.41	1.27357E-06	-23.92
177.00.00	-29.06	-118.57	-29.06	.00003	.00	2 2.85355E-02	-89.37	9.54304E-07	-23.95
178.00.00	-32.59	-122.10	-32.59	.00003	.00	2 1.90156E-02	-89.34	6.35787E-07	-23.98
179.00.00	-38.61	-128.13	-38.61	.00003	.00	2 9.50534E-03	-89.32	3.17770E-07	-24.00
180.00.00	-999.99	-999.99	-999.99	.26044	74.10	1 4.94244E-12	94.43	1.28427E-11	47.74
181.00.00	-38.61	-128.13	-38.61	.00003	.00	2 9.50534E-03	90.68	3.17762E-07	156.00
182.00.00	-32.59	-122.10	-32.59	.00003	.00	2 1.90156E-02	90.66	6.35779E-07	156.02
183.00.00	-29.06	-118.57	-29.06	.00003	.00	2 2.85355E-02	90.63	9.54296E-07	156.04
184.00.00	-26.56	-116.07	-26.56	.00003	.00	2 3.80699E-02	90.59	1.27356E-06	156.08
185.00.00	-24.61	-114.12	-24.61	.00003	.00	2 4.76237E-02	90.54	1.59383E-06	156.13
186.00.00	-23.02	-112.52	-23.02	.00003	.00	2 5.72016E-02	90.47	1.91533E-06	156.19
187.00.00	-21.67	-111.17	-21.67	.00003	.00	2 6.68082E-02	90.39	2.23833E-06	156.27
188.00.00	-20.50	-109.99	-20.50	.00003	.00	2 7.64482E-02	90.30	2.56304E-06	156.35
189.00.00	-19.47	-108.95	-19.47	.00003	.00	2 8.61259E-02	90.20	2.88972E-06	156.44
190.00.00	-18.54	-108.01	-18.54	.00003	.00	2 9.58459E-02	90.08	3.21860E-06	156.54
191.00.00	-17.69	-107.16	-17.69	.00003	.00	2 1.05612E-01	89.96	3.54989E-06	156.66
192.00.00	-16.92	-106.38	-16.92	.00003	.00	2 1.15430E-01	89.82	3.88384E-06	156.78
193.00.00	-16.21	-105.66	-16.21	.00003	.00	2 1.25302E-01	89.67	4.22064E-06	156.91
194.00.00	-15.55	-104.99	-15.55	.00003	.00	2 1.35232E-01	89.52	4.56052E-06	157.05
195.00.00	-14.93	-104.36	-14.93	.00003	.00	2 1.45225E-01	89.35	4.90367E-06	157.21
196.00.00	-14.35	-103.76	-14.35	.00003	.00	2 1.55283E-01	89.17	5.25031E-06	157.37
197.00.00	-13.80	-103.20	-13.80	.00003	.00	2 1.65411E-01	88.98	5.60061E-06	157.54
198.00.00	-13.28	-102.67	-13.28	.00003	.00	2 1.75610E-01	88.78	5.95477E-06	157.71
199.00.00	-12.78	-102.16	-12.78	.00003	.00	2 1.85885E-01	88.57	6.31295E-06	157.90
200.00.00	-12.31	-101.68	-12.31	.00003	.00	2 1.96237E-01	88.35	6.67533E-06	158.10
201.00.00	-11.86	-101.21	-11.86	.00003	.00	2 2.06670E-01	88.12	7.04206E-06	158.30
202.00.00	-11.43	-100.77	-11.43	.00003	.00	2 2.17185E-01	87.89	7.41329E-06	158.51
203.00.00	-11.02	-100.34	-11.02	.00003	.00	2 2.27784E-01	87.64	7.78917E-06	158.73
204.00.00	-10.62	-99.92	-10.62	.00003	.00	2 2.38470E-01	87.39	8.16982E-06	158.95
205.00.00	-10.24	-99.52	-10.24	.00003	.00	2 2.49242E-01	87.12	8.55537E-06	159.18
206.00.00	-9.87	-99.14	-9.87	.00003	.00	2 2.60103E-01	86.85	8.94592E-06	159.42
207.00.00	-9.51	-98.76	-9.51	.00003	.00	2 2.71052E-01	86.58	9.34157E-06	159.66

208.00 .00 -9.16 -98.39 -9.16 .00003 .00 2 2.82092E-01 86.29 9.74241E-06 159.91
 209.00 .00 -8.82 -98.04 -8.82 .00003 .00 2 2.93221E-01 86.00 1.01485E-05 160.17
 210.00 .00 -8.50 -97.69 -8.50 .00003 .00 2 3.04439E-01 85.70 1.05600E-05 160.43
 211.00 .00 -8.18 -97.36 -8.18 .00003 .00 2 3.15747E-01 85.40 1.09768E-05 160.69
 212.00 .00 -7.87 -97.03 -7.87 .00003 .00 2 3.27143E-01 85.08 1.13991E-05 160.96
 213.00 .00 -7.57 -96.71 -7.57 .00003 .00 2 3.38625E-01 84.77 1.18269E-05 161.24
 214.00 .00 -7.28 -96.40 -7.28 .00003 .00 2 3.50193E-01 84.44 1.22601E-05 161.52
 215.00 .00 -7.00 -96.09 -7.00 .00003 .00 2 3.61845E-01 84.11 1.26988E-05 161.80
 216.00 .00 -6.72 -95.79 -6.72 .00003 .00 2 3.73578E-01 83.78 1.31431E-05 162.09
 217.00 .00 -6.45 -95.50 -6.45 .00003 .00 2 3.85390E-01 83.44 1.35928E-05 162.38
 218.00 .00 -6.19 -95.22 -6.19 .00003 .00 2 3.97278E-01 83.09 1.40480E-05 162.67
 219.00 .00 -5.93 -94.94 -5.93 .00003 .00 2 4.09238E-01 82.74 1.45086E-05 162.97
 220.00 .00 -5.68 -94.66 -5.68 .00004 .00 2 4.21268E-01 82.39 1.49745E-05 163.27
 221.00 .00 -5.43 -94.39 -5.43 .00004 .00 2 4.33362E-01 82.03 1.54458E-05 163.58
 222.00 .00 -5.19 -94.13 -5.19 .00004 .00 2 4.45518E-01 81.67 1.59223E-05 163.88
 223.00 .00 -4.96 -93.87 -4.96 .00004 .00 2 4.57730E-01 81.30 1.64040E-05 164.19
 224.00 .00 -4.73 -93.62 -4.73 .00004 .00 2 4.69993E-01 80.93 1.68907E-05 164.50
 225.00 .00 -4.50 -93.37 -4.50 .00004 .00 2 4.82302E-01 80.56 1.73824E-05 164.82
 226.00 .00 -4.28 -93.12 -4.28 .00004 .00 2 4.94652E-01 80.18 1.78789E-05 165.13
 227.00 .00 -4.07 -92.88 -4.07 .00004 .00 2 5.07036E-01 79.80 1.83801E-05 165.45
 228.00 .00 -3.86 -92.65 -3.86 .00004 .00 2 5.19449E-01 79.41 1.88859E-05 165.77
 229.00 .00 -3.65 -92.41 -3.65 .00004 .00 2 5.31884E-01 79.03 1.93962E-05 166.09
 230.00 .00 -3.45 -92.19 -3.45 .00004 .00 2 5.44335E-01 78.64 1.99106E-05 166.42
 231.00 .00 -3.25 -91.96 -3.25 .00004 .00 2 5.56794E-01 78.24 2.04292E-05 166.74
 232.00 .00 -3.06 -91.74 -3.06 .00004 .00 2 5.69254E-01 77.85 2.09516E-05 167.06
 233.00 .00 -2.87 -91.53 -2.87 .00004 .00 2 5.81708E-01 77.45 2.14778E-05 167.39
 234.00 .00 -2.69 -91.32 -2.69 .00004 .00 2 5.94148E-01 77.05 2.20075E-05 167.72
 235.00 .00 -2.51 -91.11 -2.51 .00004 .00 2 6.06566E-01 76.65 2.25405E-05 168.05
 236.00 .00 -2.34 -90.90 -2.34 .00004 .00 2 6.18954E-01 76.24 2.30765E-05 168.38
 237.00 .00 -2.16 -90.70 -2.16 .00004 .00 2 6.31304E-01 75.84 2.36154E-05 168.71
 238.00 .00 -2.00 -90.51 -2.00 .00004 .00 2 6.43607E-01 75.43 2.41569E-05 169.04
 239.00 .00 -1.83 -90.31 -1.83 .00004 .00 2 6.55854E-01 75.02 2.47008E-05 169.37
 240.00 .00 -1.67 -90.12 -1.67 .00004 .00 2 6.68038E-01 74.61 2.52468E-05 169.70
 241.00 .00 -1.52 -89.94 -1.52 .00004 .00 2 6.80148E-01 74.20 2.57946E-05 170.03
 242.00 .00 -1.36 -89.75 -1.36 .00004 .00 2 6.92177E-01 73.78 2.63440E-05 170.37
 243.00 .00 -1.22 -89.57 -1.22 .00004 .00 2 7.04114E-01 73.37 2.68947E-05 170.70
 244.00 .00 -1.07 -89.40 -1.07 .00004 .00 2 7.15951E-01 72.95 2.74463E-05 171.04
 245.00 .00 -.93 -89.23 -.93 .00004 .00 2 7.27678E-01 72.53 2.79986E-05 171.37
 246.00 .00 -.79 -89.06 -.79 .00004 .00 2 7.39287E-01 72.11 2.85514E-05 171.71
 247.00 .00 -.66 -88.89 -.66 .00004 .00 2 7.50767E-01 71.70 2.91041E-05 172.04
 248.00 .00 -.53 -88.73 -.53 .00004 .00 2 7.62109E-01 71.28 2.96566E-05 172.38
 249.00 .00 -.40 -88.57 -.40 .00004 .00 2 7.73304E-01 70.86 3.02086E-05 172.71
 250.00 .00 -.28 -88.41 -.28 .00004 .00 2 7.84342E-01 70.44 3.07596E-05 173.05
 251.00 .00 -.16 -88.25 -.16 .00004 .00 2 7.95214E-01 70.02 3.13093E-05 173.38
 252.00 .00 -.04 -88.10 -.04 .00004 .00 2 8.05911E-01 69.60 3.18573E-05 173.72
 253.00 .00 .07 -87.96 .07 .00004 .00 2 8.16423E-01 69.17 3.24034E-05 174.05
 254.00 .00 .18 -87.81 .18 .00004 .00 2 8.26741E-01 68.75 3.29471E-05 174.39
 255.00 .00 .28 -87.67 .28 .00004 .00 2 8.36855E-01 68.33 3.34881E-05 174.73
 256.00 .00 .39 -87.53 .39 .00004 .00 2 8.46757E-01 67.91 3.40260E-05 175.06
 257.00 .00 .49 -87.40 .49 .00004 .00 2 8.56437E-01 67.50 3.45603E-05 175.40
 258.00 .00 .58 -87.26 .58 .00004 .00 2 8.65886E-01 67.08 3.50908E-05 175.73
 259.00 .00 .67 -87.14 .67 .00004 .00 2 8.75095E-01 66.66 3.56169E-05 176.07
 260.00 .00 .76 -87.01 .76 .00004 .00 2 8.84055E-01 66.24 3.61383E-05 176.40
 261.00 .00 .85 -86.89 .85 .00004 .00 2 8.92759E-01 65.83 3.66545E-05 176.74
 262.00 .00 .93 -86.77 .93 .00004 .00 2 9.01196E-01 65.41 3.71652E-05 177.07
 263.00 .00 1.01 -86.65 1.01 .00004 .00 2 9.09359E-01 65.00 3.76700E-05 177.41

264.00 .00 1.08 -86.53 1.08 .00004 .00 2 9.17240E-01 64.59 3.81682E-05 177.74
 265.00 .00 1.15 -86.42 1.15 .00004 .00 2 9.24829E-01 64.18 3.86596E-05 178.08
 266.00 .00 1.22 -86.31 1.22 .00004 .00 2 9.32120E-01 63.77 3.91437E-05 178.41
 267.00 .00 1.29 -86.21 1.29 .00004 .00 2 9.39104E-01 63.37 3.96201E-05 178.75
 268.00 .00 1.35 -86.11 1.35 .00004 .00 2 9.45773E-01 62.96 4.00882E-05 179.08
 269.00 .00 1.41 -86.01 1.41 .00004 .00 2 9.52121E-01 62.56 4.05476E-05 179.41
 270.00 .00 1.46 -85.91 1.46 .00004 .00 2 9.58140E-01 62.16 4.09978E-05 179.74
 271.00 .00 1.51 -85.82 1.51 .00004 .00 2 9.63822E-01 61.76 4.14384E-05 -179.92
 272.00 .00 1.56 -85.73 1.56 .00004 .00 2 9.69162E-01 61.37 4.18689E-05 -179.59
 273.00 .00 1.60 -85.64 1.60 .00004 .00 2 9.74151E-01 60.98 4.22888E-05 -179.26
 274.00 .00 1.65 -85.56 1.65 .00004 .00 2 9.78785E-01 60.59 4.26976E-05 -178.93
 275.00 .00 1.68 -85.48 1.68 .00004 .00 2 9.83056E-01 60.21 4.30949E-05 -178.60
 276.00 .00 1.72 -85.40 1.72 .00004 .00 2 9.86958E-01 59.83 4.34800E-05 -178.27
 277.00 .00 1.75 -85.33 1.75 .00004 .00 2 9.90486E-01 59.45 4.38526E-05 -177.94
 278.00 .00 1.78 -85.26 1.78 .00004 .00 2 9.93634E-01 59.07 4.42122E-05 -177.61
 279.00 .00 1.80 -85.19 1.80 .00004 .00 2 9.96398E-01 58.70 4.45581E-05 -177.28
 280.00 .00 1.82 -85.13 1.82 .00004 .00 2 9.98771E-01 58.34 4.48900E-05 -176.96
 281.00 .00 1.84 -85.06 1.84 .00004 .00 2 1.00075E+00 57.97 4.52073E-05 -176.63
 282.00 .00 1.85 -85.01 1.85 .00004 .00 2 1.00233E+00 57.61 4.55095E-05 -176.31
 283.00 .00 1.86 -84.95 1.86 .00004 .00 2 1.00350E+00 57.26 4.57962E-05 -175.98
 284.00 .00 1.87 -84.90 1.87 .00004 .00 2 1.00427E+00 56.91 4.60667E-05 -175.66
 285.00 .00 1.87 -84.85 1.87 .00004 .00 2 1.00463E+00 56.56 4.63206E-05 -175.34
 286.00 .00 1.87 -84.81 1.87 .00004 .00 2 1.00457E+00 56.22 4.65574E-05 -175.02
 287.00 .00 1.87 -84.77 1.87 .00004 .00 2 1.00409E+00 55.89 4.67766E-05 -174.70
 288.00 .00 1.86 -84.73 1.86 .00004 .00 2 1.00320E+00 55.55 4.69777E-05 -174.38
 289.00 .00 1.85 -84.70 1.85 .00004 .00 2 1.00188E+00 55.23 4.71601E-05 -174.06
 290.00 .00 1.83 -84.67 1.83 .00004 .00 2 1.00013E+00 54.90 4.73235E-05 -173.74
 291.00 .00 1.81 -84.64 1.81 .00004 .00 2 9.97962E-01 54.59 4.74673E-05 -173.43
 292.00 .00 1.79 -84.62 1.79 .00004 .00 2 9.95362E-01 54.28 4.75910E-05 -173.12
 293.00 .00 1.76 -84.60 1.76 .00004 .00 2 9.92332E-01 53.97 4.76941E-05 -172.80
 294.00 .00 1.73 -84.58 1.73 .00003 .00 2 9.88872E-01 53.67 4.77763E-05 -172.49
 295.00 .00 1.70 -84.57 1.70 .00003 .00 2 9.84980E-01 53.37 4.78370E-05 -172.19
 296.00 .00 1.66 -84.57 1.66 .00003 .00 2 9.80656E-01 53.08 4.78757E-05 -171.88
 297.00 .00 1.62 -84.56 1.62 .00003 .00 2 9.75901E-01 52.80 4.78921E-05 -171.58
 298.00 .00 1.57 -84.56 1.57 .00003 .00 2 9.70714E-01 52.52 4.78858E-05 -171.27
 299.00 .00 1.52 -84.57 1.52 .00003 .00 2 9.65097E-01 52.24 4.78562E-05 -170.97
 300.00 .00 1.47 -84.58 1.47 .00003 .00 2 9.59050E-01 51.97 4.78030E-05 -170.67
 301.00 .00 1.41 -84.59 1.41 .00003 .00 2 9.52575E-01 51.71 4.77258E-05 -170.38
 302.00 .00 1.35 -84.61 1.35 .00003 .00 2 9.45673E-01 51.45 4.76242E-05 -170.08
 303.00 .00 1.28 -84.63 1.28 .00003 .00 2 9.38347E-01 51.20 4.74979E-05 -169.79
 304.00 .00 1.21 -84.66 1.21 .00003 .00 2 9.30598E-01 50.96 4.73465E-05 -169.50
 305.00 .00 1.13 -84.69 1.13 .00003 .00 2 9.22430E-01 50.71 4.71698E-05 -169.22
 306.00 .00 1.05 -84.73 1.05 .00003 .00 2 9.13844E-01 50.48 4.69673E-05 -168.93
 307.00 .00 .96 -84.77 .96 .00003 .00 2 9.04845E-01 50.25 4.67388E-05 -168.65
 308.00 .00 .87 -84.82 .87 .00003 .00 2 8.95436E-01 50.03 4.64841E-05 -168.38
 309.00 .00 .78 -84.87 .78 .00003 .00 2 8.85621E-01 49.81 4.62029E-05 -168.10
 310.00 .00 .68 -84.93 .68 .00003 .00 2 8.75403E-01 49.60 4.58949E-05 -167.83
 311.00 .00 .57 -85.00 .57 .00003 .00 2 8.64787E-01 49.39 4.55600E-05 -167.56
 312.00 .00 .46 -85.07 .46 .00003 .00 2 8.53778E-01 49.19 4.51980E-05 -167.29
 313.00 .00 .34 -85.14 .34 .00003 .00 2 8.42380E-01 49.00 4.48088E-05 -167.03
 314.00 .00 .22 -85.22 .22 .00003 .00 2 8.30600E-01 48.81 4.43922E-05 -166.77
 315.00 .00 .09 -85.31 .09 .00003 .00 2 8.18441E-01 48.62 4.39481E-05 -166.52
 316.00 .00 -.04 -85.40 -.04 .00003 .00 2 8.05911E-01 48.44 4.34765E-05 -166.27
 317.00 .00 -.18 -85.50 -.18 .00003 .00 2 7.93014E-01 48.27 4.29773E-05 -166.02
 318.00 .00 -.33 -85.61 -.33 .00003 .00 2 7.79756E-01 48.10 4.24505E-05 -165.78
 319.00 .00 -.48 -85.72 -.48 .00003 .00 2 7.66146E-01 47.94 4.18962E-05 -165.54

320.00 .00	-.64	-85.85	-.64 .00003 .00 2 7.52187E-01	47.78 4.13143E-05 -165.30
321.00 .00	-.81	-85.98	-.81 .00003 .00 2 7.37889E-01	47.63 4.07050E-05 -165.07
322.00 .00	-.98	-86.11	-.98 .00003 .00 2 7.23256E-01	47.48 4.00684E-05 -164.85
323.00 .00	-1.16	-86.26	-1.16 .00003 .00 2 7.08297E-01	47.34 3.94046E-05 -164.62
324.00 .00	-1.35	-86.41	-1.35 .00003 .00 2 6.93019E-01	47.21 3.87138E-05 -164.41
325.00 .00	-1.55	-86.57	-1.55 .00003 .00 2 6.77429E-01	47.07 3.79962E-05 -164.19
326.00 .00	-1.76	-86.75	-1.76 .00003 .00 2 6.61535E-01	46.95 3.72521E-05 -163.98
327.00 .00	-1.97	-86.93	-1.97 .00003 .00 2 6.45344E-01	46.82 3.64817E-05 -163.78
328.00 .00	-2.20	-87.12	-2.20 .00003 .00 2 6.28865E-01	46.71 3.56853E-05 -163.58
329.00 .00	-2.43	-87.32	-2.43 .00003 .00 2 6.12105E-01	46.59 3.48633E-05 -163.39
330.00 .00	-2.68	-87.53	-2.68 .00003 .00 2 5.95072E-01	46.48 3.40160E-05 -163.20
331.00 .00	-2.93	-87.76	-2.93 .00003 .00 2 5.77775E-01	46.38 3.31440E-05 -163.02
332.00 .00	-3.20	-88.00	-3.20 .00003 .00 2 5.60221E-01	46.28 3.22475E-05 -162.84
333.00 .00	-3.48	-88.25	-3.48 .00003 .00 2 5.42420E-01	46.19 3.13271E-05 -162.67
334.00 .00	-3.78	-88.52	-3.78 .00003 .00 2 5.24379E-01	46.10 3.03833E-05 -162.50
335.00 .00	-4.08	-88.80	-4.08 .00003 .00 2 5.06108E-01	46.01 2.94167E-05 -162.34
336.00 .00	-4.41	-89.09	-4.41 .00003 .00 2 4.87614E-01	45.93 2.84278E-05 -162.18
337.00 .00	-4.75	-89.41	-4.75 .00003 .00 2 4.68906E-01	45.85 2.74172E-05 -162.03
338.00 .00	-5.10	-89.74	-5.10 .00003 .00 2 4.49994E-01	45.77 2.63856E-05 -161.89
339.00 .00	-5.48	-90.09	-5.48 .00003 .00 2 4.30885E-01	45.70 2.53336E-05 -161.75
340.00 .00	-5.88	-90.47	-5.88 .00003 .00 2 4.11589E-01	45.63 2.42619E-05 -161.62
341.00 .00	-6.30	-90.87	-6.30 .00003 .00 2 3.92115E-01	45.57 2.31713E-05 -161.49
342.00 .00	-6.75	-91.30	-6.75 .00003 .00 2 3.72470E-01	45.51 2.20626E-05 -161.37
343.00 .00	-7.22	-91.75	-7.22 .00003 .00 2 3.52665E-01	45.46 2.09364E-05 -161.26
344.00 .00	-7.73	-92.24	-7.73 .00003 .00 2 3.32707E-01	45.40 1.97937E-05 -161.15
345.00 .00	-8.27	-92.76	-8.27 .00003 .00 2 3.12607E-01	45.35 1.86352E-05 -161.05
346.00 .00	-8.85	-93.33	-8.85 .00003 .00 2 2.92372E-01	45.31 1.74618E-05 -160.95
347.00 .00	-9.48	-93.94	-9.48 .00003 .00 2 2.72012E-01	45.27 1.62744E-05 -160.86
348.00 .00	-10.16	-94.60	-10.16 .00003 .00 2 2.51536E-01	45.23 1.50740E-05 -160.78
349.00 .00	-10.90	-95.33	-10.90 .00003 .00 2 2.30952E-01	45.19 1.38613E-05 -160.70
350.00 .00	-11.71	-96.13	-11.71 .00003 .00 2 2.10269E-01	45.16 1.26375E-05 -160.63
351.00 .00	-12.62	-97.03	-12.62 .00003 .00 2 1.89498E-01	45.13 1.14033E-05 -160.57
352.00 .00	-13.63	-98.03	-13.63 .00003 .00 2 1.68645E-01	45.11 1.01599E-05 -160.51
353.00 .00	-14.78	-99.17	-14.78 .00003 .00 2 1.47721E-01	45.08 8.90821E-06 -160.46
354.00 .00	-16.11	-100.50	-16.11 .00003 .00 2 1.26735E-01	45.06 7.64922E-06 -160.42
355.00 .00	-17.69	-102.07	-17.69 .00003 .00 2 1.05694E-01	45.05 6.38397E-06 -160.38
356.00 .00	-19.62	-103.99	-19.62 .00003 .00 2 8.46090E-02	45.03 5.11348E-06 -160.35
357.00 .00	-22.11	-106.48	-22.11 .00003 .00 2 6.34881E-02	45.02 3.83879E-06 -160.33
358.00 .00	-25.63	-110.00	-25.63 .00003 .00 2 4.23403E-02	45.02 2.56095E-06 -160.31
359.00 .00	-31.65	-116.02	-31.65 .00003 .00 2 2.11746E-02	45.01 1.28100E-06 -160.30
360.00 .00	-999.99	-999.99	-999.99 .03841 .62 1 2.46193E-11	-135.79 9.82401E-13 149.94];

```

b=[1:361];
eThetaMag=[a(b,9)];
eThetaAng=[((pi/180).*(a(b,10)))];
ePhiMag=[a(b,11)];
ePhiAng=[((pi/180).*(a(b,12)))];
eThetaCos=[eThetaMag.*cos(eThetaAng)];
ePhiCos=[ePhiMag.*cos(ePhiAng)];
eThetaSin=[eThetaMag.*j.*sin(eThetaAng)];
ePhiSin=[ePhiMag.*j.*sin(ePhiAng)];
eTheta=[eThetaCos+eThetaSin];
ePhi=[ePhiCos+ePhiSin];
erhcp=eTheta+j*ePhi;
rhcpdb=20*log10(abs(erhcp)+1e-5);
theta=[0:360]';

```

```

thetaRad=(pi/180).*theta;
eT=[eTheta.^2];
eP=[ePhi.^2];
eF=[eT+j*eP];
eField=[(eF.^(.5))];
eFAbs=abs(eField);
eTAbs=abs(eTheta);
ePAbs=abs(ePhi);
figure(1)
polardb(theta,rhcpdb,'')
title(TOTAL E FIELD OF THE TELEMETRY ANTENNA (\theta=0-360, \phi=0))

```

LIST OF REFERENCES

1. David C. Jenn, "Tiny, microwave powered, remotely piloted vehicles," *IEEE Potentials*, Vol. 16, No. 5, pp. 20-22, December 1997.
2. Defense Advanced Research Projects Agency Tactical Technology Office, "Micro Air Vehicles-Toward a New Dimension in Flight." Available [Online]: <http://www.darpa.mil/tto/mav/mav_auvsi.html> [6 August 1999].
3. Narondech Suksong, "Communications Antenna for A Micro RPV," Master's Thesis, Naval Postgraduate School, Monterey, CA, March 1998.
4. Constantine A. Balanis, *Antenna Theory Analysis and Design*, Harper & Row Publishers, New York, 1982.
5. Dan's Corner of The Web, "How to become an antenna guru." Available [Online]: <<http://www.borg.com/~warrend/guru.html>> [5 May 1999].
6. John D. Kraus, *Electromagnetics*, McGraw-Hill Inc., New York, 1992.
7. Robert E. Collin, *Antennas and Radiowave Propagation*, McGraw-Hill Inc., New York, 1985.
8. Warren L. Stutzman and Gary A. Thiele, *Antenna Theory and Design*, John Wiley & Sons Inc, New York, 1981.
9. *NEC-Win Pro User's NEC Code Data Entry Manual*, Nittany Scientific, Inc., Hollister, CA, 1997.
10. David C. Jenn, "MRPV GPS and Video Antennas - Preliminary Study Design Study," Naval Postgraduate School, Monterey, CA, 1998.
11. Neus Padros, Juan I. Ortigosa, James Baker, Magdy F. Iskander, and Brace Thornberg, "Comparative study of high performance GPS receiving antenna designs," *IEEE Transactions on Antennas and Propagation*, Vol. 45, No. 4, pp. 698-706, April 1997.
12. Bradford W. Parkinson, James J. Spilker Jr., Penina Axelrad, and Per Enge, *Global Positioning System: Theory and Applications Volume I*, American Institute of Aeronautics and Astronautics, Inc., Washington, DC, 1996.
13. *Integrating GPS and Mobile Telephones-The PowerHelix GPS Antenna Datasheet*, Symmetricom, San Jose, CA, January 1999.

14. I. J. Bahl and P. Bhartia, *Microstrip Antennas*, Artech House, Norwood, MA, 1982.
15. M. D. Deshpande and N. K. Das, "Rectangular microstrip antenna for circular polarization," *IEEE Transactions on Antennas and Propagation*, Vol. AP-34, pp. 744-746, May 1986.
16. A. Adrian and D. H. Schaubert, "Dual Aperture coupled microstrip antenna for dual or circular polarization," *Electronic Letters*, Vol. 23, pp. 1226-1228, November 1987.
17. S. D. Targonski and D. M. Pozar, "Design of wideband circularly polarized aperture coupled microstrip patch antennas," *IEEE Transactions on Antennas and Propagation*, Vol. 41, pp. 214-220, February 1993.
18. C. H. Tsao, Y. M. Hwang, F. Killberg, and F. Dietrich, "Aperture coupled patch antennas with wide-bandwidth and dual polarization capabilities," *IEEE Antennas Propagation Symposium Dig.*, pp. 936-939, June 1988.
19. David M. Pozar, "A dual-band circularly polarized aperture-coupled stacked microstrip antenna for global positioning satellite," *IEEE Transactions on Antennas and Propagation*, Vol. 45, No. 11, November 1997.
20. Aromat Electronic Materials and Devices, "EMD GPS Antenna Survey." Available [Online]: <<http://www.aromat.com/emdsurveyf.htm>> [7 August 1999].
21. W. A. Johnson, D. Witton, and R. Sharpe, *PATCH Code Users' Manual*, Sandia Labs Report SAND87-2991 (limited distribution), May 1988.

INITIAL DISTRIBUTION LIST

	No. Copies
1. Defense Technical Information Center.....	2
8725 John J. Kingman Rd., Ste 0944	
Ft. Belvoir, VA 22060-6218	
2. Dudley Knox Library.....	2
Naval Postgraduate School	
411 Dyer Rd.	
Monterey, CA 93943-5101	
3. Chairman, Code IW.....	1
Information Warfare Academic Group	
Naval Postgraduate School	
Monterey, CA 93943-5121	
4. Professor David C. Jenn, Code EC/Jn.....	2
Department of Electrical and Computer Engineering	
Naval Postgraduate School	
Monterey, CA 93943-5121	
5. Professor D. Curtis Schleher, Code IW/Sc.....	2
Information Warfare Academic Group	
Naval Postgraduate School	
Monterey, CA 93943-5121	
6. Deniz Kuvvetleri Komutanligi	2
Personel Daire Baskanligi	
Bakanliklar	
Ankara, TURKEY	
7. Deniz Harp Okulu Komutanligi	1
Kutuphane	
Tuzla, Istanbul- 81704, TURKEY	
8. Emin Guven.....	2
Yuksekk Sk. Onurkent Sitesi	
D2 Blok D.3	
Kucukyali, Istanbul-81570, TURKEY	

No. Copies

9. Gary Lee 1
Lutronix Corp.
13627 Portofino Dr.
Del Mar, CA 92014